

# A component based modular treatment of the soil-plant-atmosphere continuum: the GEOSPACE framework (v.1.2.9)

Concetta D'Amato<sup>1,2</sup>, Niccolò Tubini<sup>2</sup>, and Riccardo Rigon<sup>1,2</sup>

<sup>1</sup>Center Agriculture Food Environment - C3A, University of Trento, Trento, Italy

<sup>2</sup>Department of Civil, Environmental and Mechanical Engineering - DICAM, University of Trento, Trento, Italy

**Correspondence:** Concetta D'Amato (concettadamato94@gmail.com)

**Abstract.** The soil-plant-atmosphere continuum (SPAC) system is a complex and interconnected network of physical phenomena, encompassing heat transfer, evapotranspiration, precipitation, water absorption, soil water flow, substance transport, and gas exchange. These processes govern the exchange of energy **C21** matter, and water within the SPAC system. **C22 Modeling the SPAC system involves multiple disciplines, including hydrology, ecology, and computational science, making a physically-based approach inherently interdisciplinary and essential for capturing the complexity of the system.** To better understand and model SPAC interactions, interdisciplinary approaches are essential due to the inherent complexity of the system. Instead of relying on a single monolithic model, we propose a component-based modeling approach, where each component addresses a specific aspect of the system. Object-oriented programming (OOP) is adopted as the foundational framework for this approach, providing flexibility and adaptability to accommodate the ever-changing nature of the SPAC system.

10 The present study introduces ~~In this paper,~~ the Soil Plant Atmosphere Continuum Estimator in GEOframe (GEOSPACE) ~~is presented,~~ **a new ecohydrological modeling framework** in particular its one-dimensional development, GEOSPACE-1D. **C2-C9 GEOSPACE leverages and extends selected components from the GEOframe modeling system, while also integrating newly developed modules, to comprehensively simulate water transport dynamics in the SPAC system.** The framework of **GEOSPACE-1D** is a tool designed to facilitate robust, reliable and transparent simulations of SPAC interactions. It embraces 15 the principles of open-source software and modular design, aiming to promote open, reusable, and reproducible research practices. Instead of relying on a single monolithic model, we propose a component-based modeling approach, where each component addresses a specific aspect of the system. Object-oriented programming (OOP) is adopted as the foundational framework for this approach, providing flexibility and adaptability to accommodate the ever-changing nature of the SPAC system. ~~By implementing the OOP, GEOSPACE-1D breaks down the complexity of SPAC modeling into smaller, self-contained~~ 20 ~~structures, each responsible for a specific scientific or mathematical concept. This modular architecture adheres to the "open to extensions, closed to modifications" philosophy, enabling easy model extension without disrupting existing components. Equations are implemented in an abstract manner, emphasizing the use of common interfaces over concrete classes, a hallmark of contemporary OOP. GEOSPACE-1D adopts a generic programming framework, where distinct classes adhere to a common interface. This compartmentalization serves two critical purposes: validating individual processes against analytical solutions~~ 25 ~~and facilitating the integration of novel processes into the system.~~

The paper emphasizes the significance of modeling the coupling between infiltration and evapotranspiration **C23**through two "virtual" simulations based on real-world input data from the "Spike II" experiment, to explore for accurate hydrological simulations. It explores the interplay between plant transpiration, soil evaporation, and soil moisture dynamics, highlighting the need to account for these interactions in SPAC models. The paper concludes by underlining the importance of modularity, transparency, and openness in SPAC modeling, principles that underlie the development of GEOSPACE-1D and its components. Overall, GEOSPACE-1D represents an approach to SPAC modeling, providing a flexible and extensible framework for studying complex interactions within the Earth's Critical Zone. It is worth recalling that the fundamental premise of GEOSPACE-1D is not to create a single soil-plant-atmosphere model, but to establish a system that allows the creation of a series of soil-plant-atmosphere models, adapted to the specific needs of the user's case study.

35 *Copyright statement.*

## 1 Introduction

The Soil-Plant-Atmosphere Continuum (SPAC) encompasses a wide range of interconnected physical phenomena, including heat transfer, evapotranspiration, precipitation, water absorption and infiltration, soil water flow, substance transport, and gas exchange, all of which influence the exchange of energy, matter, and water among these three compartments (Fisher and Koven, 2020; Blyth et al., 2021; Li et al., 2021). A variety of formulations for the underlying physics of these processes are currently debated, including soil-root interactions (Steudle, 2000; Schröder et al., 2008; Manoli et al., 2017), alternative formulations for plant hydraulics (Verhoef and Egea, 2014b; Silva et al., 2022; Giraud et al., 2023), constraints imposed by water-limited availability (water stress) and their combinations (Lhomme, 2001; Verhoef and Egea, 2014b), the characterization of soil properties in the presence of roots (York et al., 2016; Carminati and Javaux, 2020), and coupling plant behavior with atmospheric transport (Katul et al., 2001; Poggi et al., 2004; Mauder et al., 2020; Finnigan et al., 2009). Additional discussions include the statistical description of plant canopies (Kerches Braghieri, 2018; McGrath et al., 2016), individual plant traits (Mencuccini et al., 2019; Cranko Page et al., 2024), and the interactions between trees, soil microbiology (Cassiani et al., 2015; Simard et al., 1997), and atmospheric processes (Brunet, 2020). Depending on specific objectives and the temporal and spatial scales of analysis, various simplifications of these processes are often employed (Anderson et al., 2003; Donovan and Sperry, 2000).

Given the complexity of the SPAC domain, numerous modeling approaches have been developed. These include physically based models (PBM) (Fatichi et al., 2016) and those leveraging statistical learning techniques, such as machine learning (ML) (Pal and Sharma, 2021). Traditional PBM-based land surface models, widely used in hydrology and agronomy, often employ simplified governing equations, such as the Penman-Monteith equation (Pereira et al., 2015) or the Priestley-Taylor approach (Formetta et al., 2014). More advanced SPAC models include SVAT (Soil-Vegetation-Atmosphere Transfer) models and LSM (Land Surface Models). While SVAT models focus on vegetation-related processes and LSMs cover a broader range

of processes, the distinction between these categories is not always clear-cut (Blyth et al., 2021; Fisher and Koven, 2020; Pal and Sharma, 2021). C19 For a comprehensive model overviews, we recommend Blyth et al. (2021) for LSM comparisons, Fatchi et al. (2016) for process-based model capabilities, and Bonan et al. (2024) for Earth System modeling perspectives. 60 Additional valuable references offering complementary perspectives include Overgaard et al. (2006), McDermid et al. (2017), Vereecken et al. (2019), Bierkens (2015) and Miralles et al. (2025). These references collectively indicate that achieving a deeper understanding and accurate modeling of SPAC interactions requires highly interdisciplinary approaches which, in our assessment, necessitates moving beyond the traditional notion of "model."

To address the implementation challenges arising from the complexity of SPAC processes and the diversity of possible 65 solutions, the literature advocates dividing software into self-contained, independent components interconnected through a supporting software layer. This approach, known as "Modeling by Components" (MBC), has been in use for over forty years (Holling, 1978) and was initially developed to integrate knowledge across disciplines (Moore and Hughes, 2017). In recent decades, MBC has gained significant importance within environmental modeling (Argent, 2004; Serafin, 2019). Notable MBC implementations in hydrology and meteorology include frameworks as TIME (Rahman et al., 2003), CSDMS (Peckham et al., 70 2013), ESMF (Collins et al., 2005), OMS (David et al., 2013), and RAVEN (Craig et al., 2020). A more extensive list can be found in Chen et al. (2020).

True MBC systems adopt a service-oriented architecture (SOA) (Richards and Ford, 2020), which facilitates the integration of heterogeneous data sources. SOA frameworks are inherently scalable, designed to operate across diverse machines and architectures, and are fundamental to the infrastructure of the Digital Earth.(Rigon et al., 2022; David et al., 2013). By 75 abstracting computational details, SOA enables users to focus on modeling rather than the complexities of the underlying computational engines. Despite the advantages of MBC concepts, practical implementation remains challenging. It often requires programmers to adopt new workflows and habits. The OMS framework has explicitly addressed these challenges, bridging the gap between conceptual elegance and practical usability (Lloyd et al., 2011). These frameworks aim to meet broader scientific needs while adhering to good scientific practices, as outlined in Rigon et al. (2022).

To our knowledge, no existing SVAT or LSM models implement a true MBC structure, although some exhibit highly modular 80 software organization. Beyond leveraging MBC, incorporating internal modularity through Object-Oriented Programming (OOP) principles is equally important, as emphasized by Rouson et al. (2014) and Gardner and Manduchi (2007). OOP promotes code reuse, improves readability, and enhances efficiency and scalability. Moreover, employing appropriate levels of abstraction, as theorized by Berti (2000), enhances model adaptability and reliability while minimizing the need for modifications to existing code.

These principles, C19-24 which we have found inadequately implemented in previous modeling efforts, have guided the development of a new ecohydrological modeling framework within GEOframe, GEOSPACE, the Soil-Plant-Atmosphere Continuum Estimator in GEOframe, which we present in this paper. This software platform integrates MBC concepts with OOP 90 principles to transcend traditional modeling paradigms, focusing on the interactions and feedback mechanisms within the SPAC. C19-C24 The MBC approach maintains complete control over code evolution while creating a unified framework applicable to eco-hydrological, agro-meteorological, and hydro-climatological communities. In developing GEOSPACE, we have

prioritized strict adherence to FAIR principles (Findable, Accessible, Interoperable, and Reusable) (Wilkinson et al., 2016) to ensure openness and availability. Additionally, we address specific algorithmic limitations identified in similar software, particularly regarding inadequate treatment of transitions between saturated and unsaturated conditions and the implementation of appropriate numerical solvers. C2-C3-C10-C27-C30 The GEOSPACE framework functions as an integral component of the GEOframe system and it uses some of the components available in GEOframe to simulate the water transport in the continuum SPAC, thus being the ecohydrological model of GEOframe. GEOframe is an open-source, component-based hydrological modelling system (Formetta et al., 2014; Bancheri et al., 2020). Rather than being a single model, GEOframe is a modular framework, where each part of the hydrological cycle is implemented in a self-contained building block, an OMS3 component (David et al., 2013). Models available in GEOframe cover a wide range of processes, including geomorphic and DEM analysis, spatial interpolation of meteorological variables, radiation budget estimation, infiltration, evapotranspiration, runoff generation, channel routing, travel time analysis, and model calibration. It allows users to build custom modeling solutions to address various hydrological challenges. The GEOSPACE framework presented here was developed by composing and extending existing GEOframe components: WHETGEO (Water Heat and Transport) (Tubini and Rigon, 2022), GEOET (EvapoTranspiration), and BrokerGEO, to simulate complex soil-vegetation-atmosphere interactions in the Critical Zone. While GEOSPACE builds upon existing components in GEOframe, this work contributes three main innovations: (i) the development of GEOET, a new evapotranspiration module evolved from the established ETP-GEOframe component (Bottazzi, 2020); (ii) the implementation of BrokerGEO, a new coupler component enabling the dynamic interaction between evapotranspiration and infiltration processes; (iii) the extension of WHETGEO (Tubini and Rigon, 2022) to allow modular and seamless coupling with GEOET and BrokerGEO. These contributions represent both algorithmic and structural advances over previous models, such as the monolithic GEOtop framework (Rigon et al., 2006), and establish GEOSPACE as the ecohydrological core of GEOframe.

This paper is organized as follows: Section 2 provides an overview of the GEOSPACE system and its hierarchical software architecture. Sections 3, 4, and 6 introduce its main components: WHETGEO, GEOET, and BrokerGEO. Section 5 discusses the implementation of the stress function, addressing evapotranspiration constraints caused by water scarcity or other environmental factors. Each section C8 follows a similar structure and includes a concise overview of the mathematical equations employed and relevant software implementation details. Readers less interested in the informatics can skip the latter portions of these sections. Section 7 presents a use case, followed C9 two "virtual" simulations based on real input data to showcase the potential applications and capabilities of the coupled system of GEOSPACE-1D and verify its correct functioning. In addition, a dedicated subsection describes general model inputs and outputs in detail. Finally, Section 8, which describes the availability of the code, executables, training materials, fair use conditions, and concludes the paper.

While this paper does not delve into the rationale behind the implemented physics, which is addressed in other contributions, it focuses on software organization and the integration of components into a cohesive modeling solution. This approach, by introducing feedback mechanisms, transcends traditional modeling paradigms to become more than a single model with boundary conditions (Staudinger et al., 2019). Appendices provide technical details, and supplementary materials include notebooks for data preparation, output visualization, and video tutorials.

## 2 GEOSPACE-1D System Overview and its perceptual model

The framework presented here, the Soil-Plant-Atmosphere Continuum Estimator in GEOframe (GEOSPACE), is an ecohydrological framework within the GEOframe system. It is designed to simulate interactions within the soil-plant-atmosphere continuum and analyze processes occurring in the Earth's Critical Zone (CZ) (National Research Council et al., 2001). GEOSPACE-1D models the mass and energy budgets as well as water flow along a soil column, accounting for water uptake by vegetation as evapotranspiration flux (ET).

As outlined in the Introduction, the framework offers multiple alternatives for simulating key physical processes (e.g., evapotranspiration, stress factor computations, soil parameterizations) with varying levels of complexity and detail. This flexibility allows users to tailor the model to their specific case studies, compare different formulations, and easily add new features. Such modularity enhances the reliability of modeling solutions by enabling the integration of appropriate components. The component-based structure of GEOSPACE-1D also improves software robustness and facilitates third-party testing and inspection. Moreover, the software is open source and adheres to modern software engineering practices (Rigon et al., 2022). The OMS3 workflow is recorded in ".sim" files, ensuring that any deterministic simulation can be precisely replicated. GEOSPACE-1D prioritizes the development of reliable, robust, and replicable models, as emphasized in Prentice et al. (2015). Its flexibility allows for varying degrees of realism by selecting or developing components aligned with modeling objectives and advancements in research.

Based on the principles of Tubini et al. (2021), the implementation of the basic equations of GEOSPACE-1D is abstract. The equations describing the processes inherit from a common interface, following the principle of "programming to interfaces, not to concrete classes." These equations are organized into libraries that streamline the implementation of partial differential equations (PDEs), ordinary differential equations (ODEs), and other equation types with flexibility and minimal effort.

While the ultimate goal is to comprehensively cover all compartments of the SPAC, this paper primarily focuses on water and energy exchanges between soil, plants, and atmosphere, with a reasonable treatment of canopies. The GEOframe system already includes a wide array of ODE-based models for some of these exchanges. However, GEOSPACE-1D specifically incorporates PDEs, particularly for the soil compartment. It features a robust implementation of the Richards-Richardson equation (Tubini et al., 2021; Casulli and Zanolli, 2010) for 1D soil water flow and extends the Penman-Monteith approach for transpiration (Schymanski and Or, 2017; Bottazzi et al., 2021). Additionally, ancillary components have been developed for radiative transfer based on Ryu et al. (2011) and de Pury (1995), and for coupling the water budget with the energy budget and solute transport in the soil.

GEOSPACE-1D comprises a coupled model consisting of three primary components: WHETGEO, GEOET, and BrokerGEO. WHETGEO, Water Heat and Transport in GEOframe (Tubini and Rigon, 2022), solves the conservative form of Richardson-Richards equation using the Newton-Casulli-Zanolli algorithm (Casulli and Zanolli, 2010), and also implements a numerical solution to solve the transport equation adopting the algorithm presented in Casulli and Zanolli (2005).

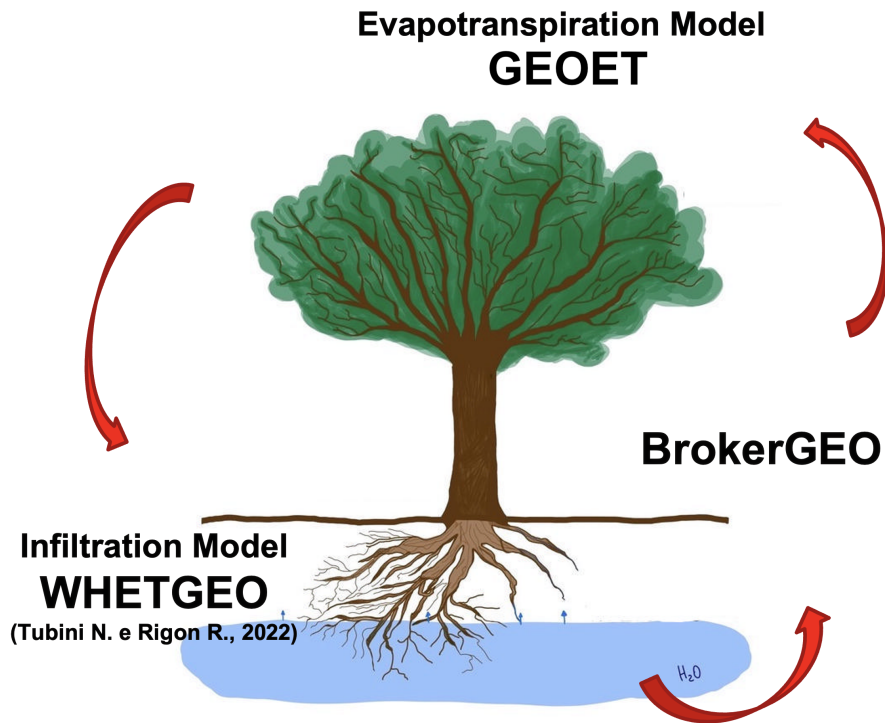


**Figure 1.** GEOSPACE-1D cycle path: Presented graphically (designed by D'Amato C.) is the cyclic operation of GEOSPACE-1D, highlighting the crucial linkage among its three components. This feedback mechanism plays a key role in ensuring the mass and energy balance throughout the system.

GEOET (GEOframe EvapoTranspiration) is a suite of models that is designed to implement different formulations of ET, from the simplest Priestley-Taylor (PT) formula (Priestley and Taylor, 1972) to the complex computation of the energy budget at the canopy scale, as described in D'Amato and Rigon (2025).  
160

Currently GEOET, in addition to PT, incorporates the Penman-Monteith FAO model (PM-FAO) and the GEOframe-Prospero model (Bottazzi, 2020; Bottazzi et al., 2021). It is also designed to integrate more complex models that account for plant hydraulics, being implemented according to D'Amato and Rigon (2025). The presence of multiple models for computing evapotranspiration within a unified framework enables a comprehensive comparison of models and parameterizations, as they can leverage common auxiliary components. This possibility also meets the needs of users by offering a selection of modelling approaches of different level of complexity, allowing users to choose according to their specific needs and available data. GEOET is also designed to implement the multiple water and environmental stress functions mentioned in the introduction, which are currently based on the Jarvis model (Macfarlane et al., 2004) and the Medlyn stomatal conductance model (Medlyn et al., 2011; Ball et al., 1987; Lin et al., 2015). Furthermore, GEOET models depth growth and root density functionally to understand soil-plant interactions in the process of root water uptake.  
165  
170

Finally, BrokerGEO is the coupler that allows the exchange of data between the other two components in memory, splits evaporation ( $E_s$ ) and transpiration ( $E_t$ ) between the control volumes in which the soil column is discretized.

The operational flow of the model follows a cyclic pathway, as illustrated in Figure 1. Starting with WHETGEO-1D, GEOSPACE-1D computes the water suction for each control volume within the soil column. This information, integrated  
175 into the GEOET-StressFactor modules (further described in Section 5), plays a crucial role in determining the reduction in ET for each control volume, which is then consolidated into a global water stress factor value.

Furthermore, the GEOET-StressFactor modules incorporate additional reductions in ET associated with environmental variables, including air temperature, net radiation, and vapor pressure deficit, when necessary, in accordance with the selected method. The specific manner in which these stress factors are utilized varies depending on the chosen method or ET model, as  
180 detailed in Section 4, with the objective of limiting water abstraction from the soil.

Subsequently, BrokerGEO is responsible for partitioning the global AET into the soil control volumes using a root functioning model. Finally, an iterative process begins, during which WHETGEO, informed by the water evapotranspired from each control volume, recalculates the soil water potential, ensuring the conservation of both mass and energy budgets.

## 2.1 General notes about the software organization of GEOSPACE-1D

185 The macro conceptual structure of GEOSPACE-1D is mirrored in a hierarchy of software entities. At a higher level are the OMS3 components (David et al., 2013, 2014). OMS3 is a component-based environmental modeling framework that empowers developers to create distinct components for individual modeling concepts. These components can be, in principle executed and tested independently, thus establishing what could be called a secondary level of concern. A graphical example of a component is illustrated in Figure 2. Each input parameter is sourced from a reader component or another component if derived  
190 from some modelling, while each output parameter is handled by a writer component. This setup facilitates straightforward management of data formats, streamlining the process for ease of use. Leveraging the modularity of OMS3, GEOSPACE-1D components integrate at runtime by connecting them with the OMS3 DSL language based on Groovy (<https://groovy-lang.org>, last accessed: December 19, 2024). A standard operational configuration of the GEOSPACE-1D OMS3 components during runtime is depicted in Figure 3, with simplification achieved by omitting all input/output connections for clarity.

195 The GEOSPACE-1D system depicted in Figure 3 consists of three main interconnected parts, each comprising a set of related components. WHETGEO actually has multiple variants, each distinguished by unique capabilities outlined in Tubini and Rigon (2022). More intricate is the GEOET, comprising five distinct components, each tasked with specific functions such as stress factor estimation, roots modeling, soil evaporation estimation, and transpiration computation using, in this case, the Prospero model. Alternatively, a single component can replace the latter two and the one estimating the total evapotranspiration by employing, for instance, the Priestley-Taylor formula to estimate comprehensive evapotranspiration values. BrokerGEO employs  
200 two components in its connector role. The arrows denote variable flow among components, with thickness reflecting the volume of exchanged variables. C4-C20 For a comprehensive understanding of the complete workflow, we direct readers to examine the simulation configuration files provided in the supplemental material, particularly the `geospacelD_ProseroPM.sim` file. These `.sim` files, a standard feature of the OMS framework, serve as executable documentation that precisely records the

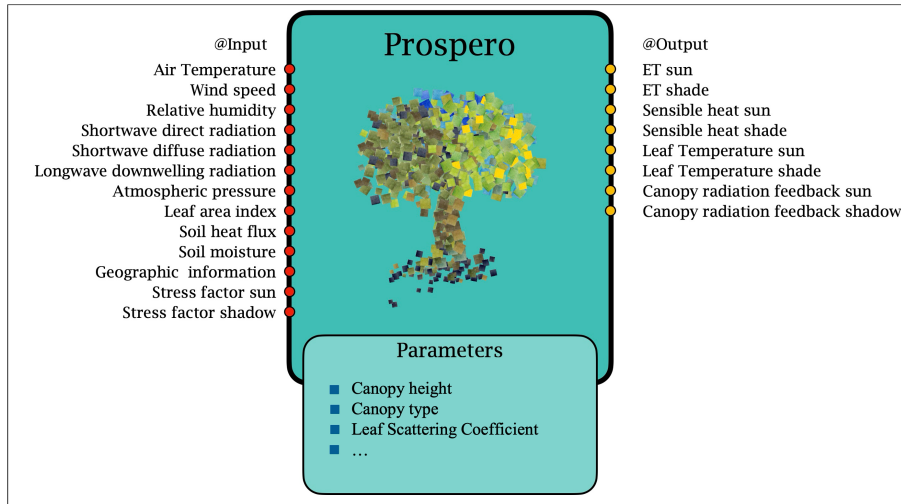


**Figure 2.** A pictorial representation of the Prospero OMS3 component with most of its inputs and outputs.

205 **model workflow, component connections, and parameter settings. The supplemental material also includes a concise presentation with accompanying slides that provide detailed guidance on interpreting .sim file structure, component relationships, and execution sequence, offering valuable insights for both new users and those seeking to modify existing simulations.**

OMS3, beyond the components, offers essential services, including tools for calibration and implicit parallelization of component runs. Further insights into the framework are available in the Supplemental material.

210 Deeper within the software, written in Java programming language, it is organized into packages that encapsulate cohesive functional modules. The names of the packages formed are as follows:

`it.geoframe.blogspot.modelname.packagename`

and are designed from being confused with that of other models in the literature that implement the same classes. The site <https://geoframe.blogspot.com/> is the blog where all the news and material about GEOframe are posted and the uniqueness of the URL guarantees that the name of the packages and classes are unique over the web. The contents of these packages are illustrated, for each of the three compartments, in the following sections.

220 A few software engineering choices were made and are characteristic “patterns” of the programming in GEOframe. Classes represent the finer programming level. In fact, internally, GEOSPACE-1D is coded with the Java language by organizing the various classes between interfaces and abstract classes. This adheres to the object-oriented principle “program to interfaces, not concrete classes,” facilitating the creation of scalable and maintainable software solutions. As stated earlier, re-usability of the Java code is one of the prerogatives of the model. Therefore, we have adopted a generic programming approach (Berti, 2000) of decoupling the concrete data representation from the algorithm implementations, by balancing it with specific approaches to improve the computational efficiency of the software. Because of these special programming structures, “patterns”, are often

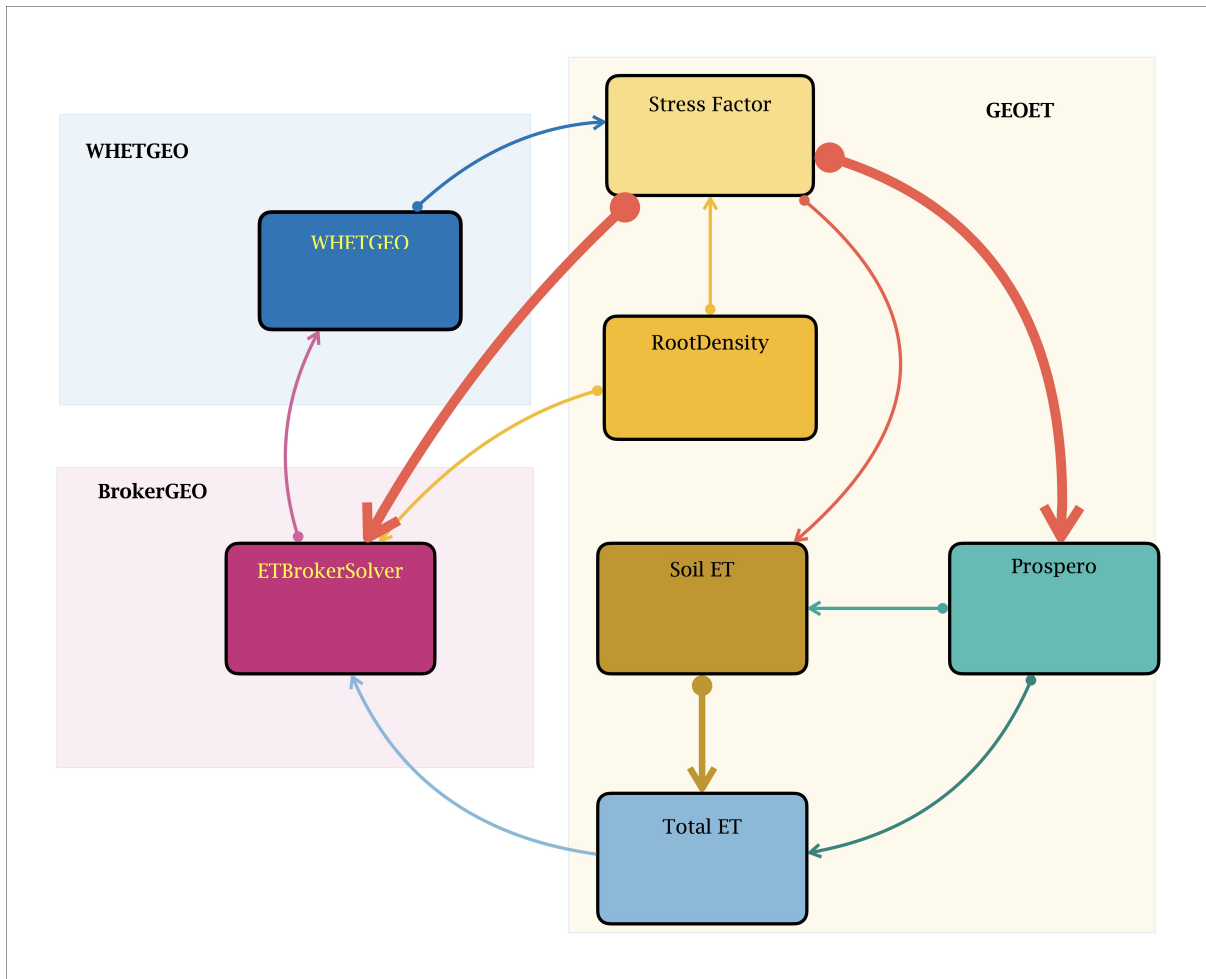


**Figure 3.** Here is an illustration of a simplified configuration in GEOSPACE-1D, focusing on component organization. We have omitted the components responsible for file I/O. One of the components, WHETGEO, exemplifies the various possibilities, differing in whether they account for the influence of the energy budget on flow. C4-C20 The simulations, as described in the text, begin with the WHETGEO component and progress according to the directional flow indicated by the arrows. The thickness of each arrow represents the number of variables exchanged between components, providing a visual indication of data transfer magnitude between system elements. For getting the complete information about the workflow, please refers, for instance to the `geospace1D_ProspéroPM.sim` which can be found in the supplemental material.

used. In particular the so called `Factory Pattern` (Gamma et al., 1995) is used to instantiate at run time the concrete  
225 classes chosen by the user among the various possibilities.

Because we are mostly interested in the implementation issues in this paper, it merits to acknowledge a crucial aspect for  
facilitating information exchange between the soil and atmospheric compartments which is how the data classes, i.e. the Java  
classes that manage the data quantities, are defined. These include:

- `ProblemQuantities`
- 230 - `InputTimeSeries`
- `Parameters`

These data classes serve as data containers and are managed distinctively from conventional OOP practices, but similar to  
traditional scientific programming. They are mutable singleton static classes, instantiated once and serving as repositories for  
data updated at each time step. Further elaboration on these classes will be provided in the following sections.

### 235 3 WHETGEO

The first pillar of the GEOSPACE-1D modeling system is WHETGEO (Tubini and Rigon, 2022; Tubini et al., 2021). Its 1D  
deployment, WHETGEO-1D is a new physically based model, simulating the water and energy budgets in a soil column.  
It solves the conservative form of Richardson-Richards equation,  $R^2$ , (Richards, 1931; Richardson, 1922) using the Newton-  
Casulli-Zanolli (NCZ) algorithm (Casulli and Zanolli, 2010) and also implements the numerical solution to solve the advection-  
240 dispersion equation adopting the algorithm presented in Casulli and Zanolli (2005), currently applied to the heat transport.  
More comprehensive information about WHETGEO can be found in Tubini (2021), Tubini and Rigon (2022) and Tubini et al.  
(2021).

WHETGEO delves into infiltration and soil moisture dynamics that have cascading effects on various aspects of the envi-  
ronment, water resources, accurate water balance estimation, aquifer recharge prediction and flow patterns.

245 For what regards evaporation, it is well-established that plant productivity is significantly influenced by the patterns of soil  
moisture dynamics (Porporato et al., 2004). Soil moisture deficit, in particular, reduces plant water potential, inducing wa-  
ter stress, which can lead to dehydration, loss of turgor, xylem cavitation, stomatal closure, and a decrease in photosynthesis  
(Nilsen and Orcutt, 1996). At the same time, it is an oversimplification to model soil moisture dynamics without considering  
transpiration, which constitutes a significant portion of the water budget. The relationship between soil moisture and evapo-  
250 transpiration is a crucial component for accurately representing soil water balance. Regardless of the specific ET model used,  
it is the amount of water extracted from the soil at various depths by plant roots (Evaristo and McDonnell, 2017). These roots  
are capable of absorbing substantial amounts of water, significantly altering the distribution of the water column.

An approach to include the evapotranspiration flux within the soil moisture dynamics is to add a sink term representing water  
extraction by plant roots in the  $R^2$  equation, obtaining a modified one-dimensional continuity equation (Feddes et al., 1976;  
255 Molz, 1981):

$$\frac{\partial \theta}{\partial t} + S_s \frac{\theta}{\theta_s} \frac{\partial \psi}{\partial t} = \nabla \cdot (K(\theta) \nabla (\psi + z)) - S(z) + R(z) \quad (1)$$

where the forces acting are gravity  $z$  [L], and the matric potential  $\psi$  [L]. In Eq. 1,  $K$  [ $LT^{-1}$ ] is the hydraulic conductivity;  $\theta$  [-] is the dimensionless volumetric water content;  $\nabla$  [ $L^{-1}$ ] is the gradient operator;  $z$  [L] is the vertical coordinate, positive upward,  $S$  is the water extraction function [ $T^{-1}$ ], and  $R$  [ $T^{-1}$ ] is the water redistribution function by roots. The function  $S(z)$  represents water extraction by plant roots and can depend on space, time, root-density distribution, water potential, water content, or a combination of these variables (Feddes et al., 1976; Perrochet, 1987; Lai and Katul, 2000).  $S_s$  [ $L^{-1}$ ] is the specific storage coefficient, defined as

$$S_s := \rho g (n\beta + \alpha) \quad (2)$$

with  $\rho$  [ $ML^{-3}$ ] being the water density,  $g$  [ $LT^{-2}$ ] is the gravitational acceleration,  $n$  [ $L^3L^{-3}$ ] is the soil porosity,  $\beta$  [ $LT^2M^{-1}$ ] is the liquid compressibility, and  $\alpha$  [ $LT^2M^{-1}$ ] is the soil matrix compressibility.

Molz and Remson (1970) highlight the impracticality of modeling water transport in soil with complex root systems considering flow to individual rootlets. Precise root geometry is hard to measure and varies over time. Additionally, root water permeability changes along their length, noted by Kramer (1970). Consequently, the extraction functions  $S(z)$  is treated with simplified models which adopt a macroscopic, not microscopic approach, which is actually computed by the BrokerGEO components (described in section 6).

As the source term models, the roots themselves, are capable of redistributing water between different soil layers (Beyer et al., 2018) but the modelling of the source term  $R(z)$  is not under scrutiny in this paper.

### 3.1 Extension of the Richards Solver, i.e. on the RichardsRootSolverMain

The algorithmic concepts of WHETGEO are comprehensively described in Tubini and Rigon (2022), but here, we summarize only those aspects, which are related to the extension we made for allowing the connection with GEOET and BrokerGEO.

In WHETGEO, the column of soil is discretized in layers, parts of the soil column with the same soil type, and control volumes, finite-volume elements, in which the  $R^2$  equation is solved. Each control volume is characterized by geometrical quantities, a parameter set, containing all the parameters that control the dynamics of the flow, the form of the equations to be solved, which are specific for each control volume. All of this information is stored in the grid file and, once read, is stored in the `Geometry` and `ProblemQuantities`, singleton classes as illustrated in Figure 4.

Upon a more detailed examination of Figure 4 reveals that `ProblemQuantities` and `Geometry` are typical example of "reflexive association", a type of relationship between elements in a class diagram where an element is associated with itself. In other words, it is an association between instances of the same class and it means that the class could work stand-alone. The term  $S(z)$  in Eq. 1 is a sink which affects any layer and this can be obtained by means of the introduction of some new classes.

The first class that has been added is:

- `ComputeQuantitiesRichardsRoot`

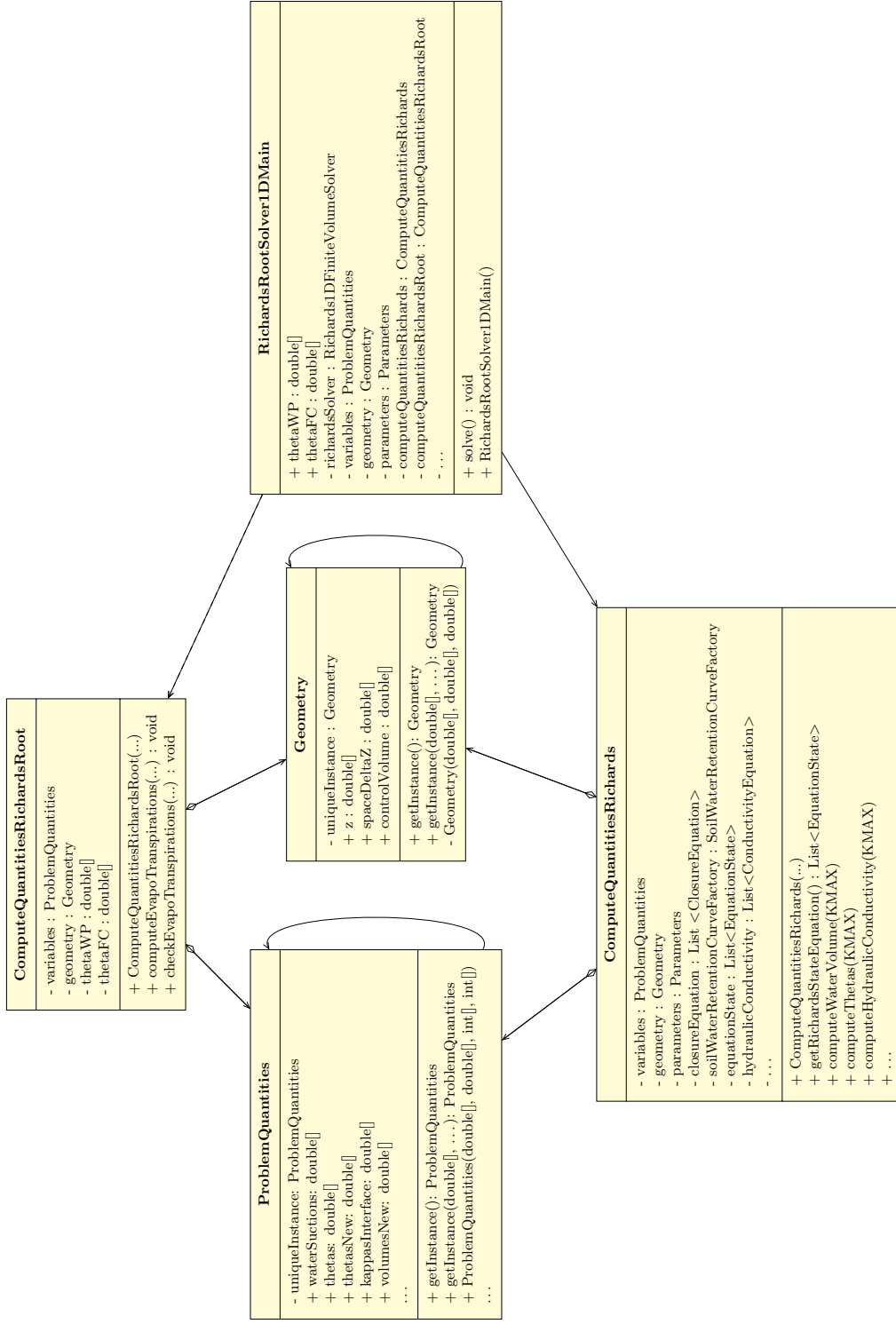


**Figure 4.** UML class diagram for the RichardsRootSolverIDMain class. The class solves Eq. 1 directly calling the methods of the concrete classes ComputeQuantitiesRichardsRoot and ComputeQuantitiesRichards.

ComputeQuantitiesRichardsRoot is a java class with the responsibility of managing the evapotranspiration demand for each control volume, sourced from BrokerGEO. Its primary function involves assessing the requested water volume against the available water content in each control volume, thereby estimating the reduction in ET and deriving a stress factor,  $g_{w_i}$ ,  
290 for every soil layer. These stress factors are subsequently utilized iteratively to determine the actual evapotranspiration (AET) through information exchange with GEOET via BrokerGEO. AET is then deducted from each control volume, with the class overseeing algorithm convergence as well.

A closer inspection of Figure 4 reveals that the ComputeQuantitiesRichardsRoot class is composed by aggregation with the ProblemQuantities class and the Geometry class as mentioned above. The first one contains all the variables  
295 of the models and its implementation using the singleton pattern (Freeman et al., 2008), whereas, the second one manages the geometric features of the grid and how grid elements are connected to each other.

While the present deployment of GEOSPACE works in a 1D column, however it is ready to manage the more complex topologies of a 2D or a 3D future versions of the system.

The relationship between the classes ComputeQuantitiesRichardsRoot and ProblemQuantities can be de-  
300 scribed as a combination of both "association" and "aggregation" (Fowler, 2004). The ComputeQuantitiesRichardsRoot class maintains a reciprocal "association" with the ProblemQuantities class through the instantiated variables allowing them to interact and exchange information. Furthermore, an "aggregation" relationship exists where the ComputeQuantitiesRichardsRoot class encapsulates an instance of the ProblemQuantities class to manage and compute various problem-related quantities as is illustrated by an empty diamond shape (Figure 4). Overall, this relationship structure enhances the mod-  
305 ularity and organization of the software design, enabling the ComputeQuantitiesRichardsRoot class to efficiently utilize and manage the data provided by the ProblemQuantities class.

The class involved in solving Equation 1 considering the amount of water removed by evapotranspiration is the concrete class, RichardsRootSolver1DMain, as shown in the UML diagram of Figure 4.

The RichardsRootSolver1DMain class, as shown in Figure 4 is directly connected with ComputeQuantitiesRichards-  
310 Root and ComputeQuantitiesRichards and with their methods to compute the solution of the pressure value  $\psi$  at any time step. In this specific case, the RichardsRootSolver1DMain class uses the ComputeQuantitiesRichardsRoot and the actual solver is the solve() method which contains the solving algorithms. This abstract structure allows with the change of each of the "Compute" classes to change the solver type by just adding some new class in substitution.

## 4 GEOET

315 The process of plant transpiration propels the exchange of water and energy between the Earth's surface and the atmosphere (Katul et al., 2012). This phenomenon significantly impacts the uptake of carbon by ecosystem and also plays a pivotal role in determining how rainfall infiltrates into the soil and the moisture profile dynamic. In fact, the interaction between soil evaporation and plant transpiration is not merely a sum of physical processes, but is influenced by feedback mechanisms. As plants transpire, they create a suction that draws moisture from the soil into their root systems, thereby influencing the rate

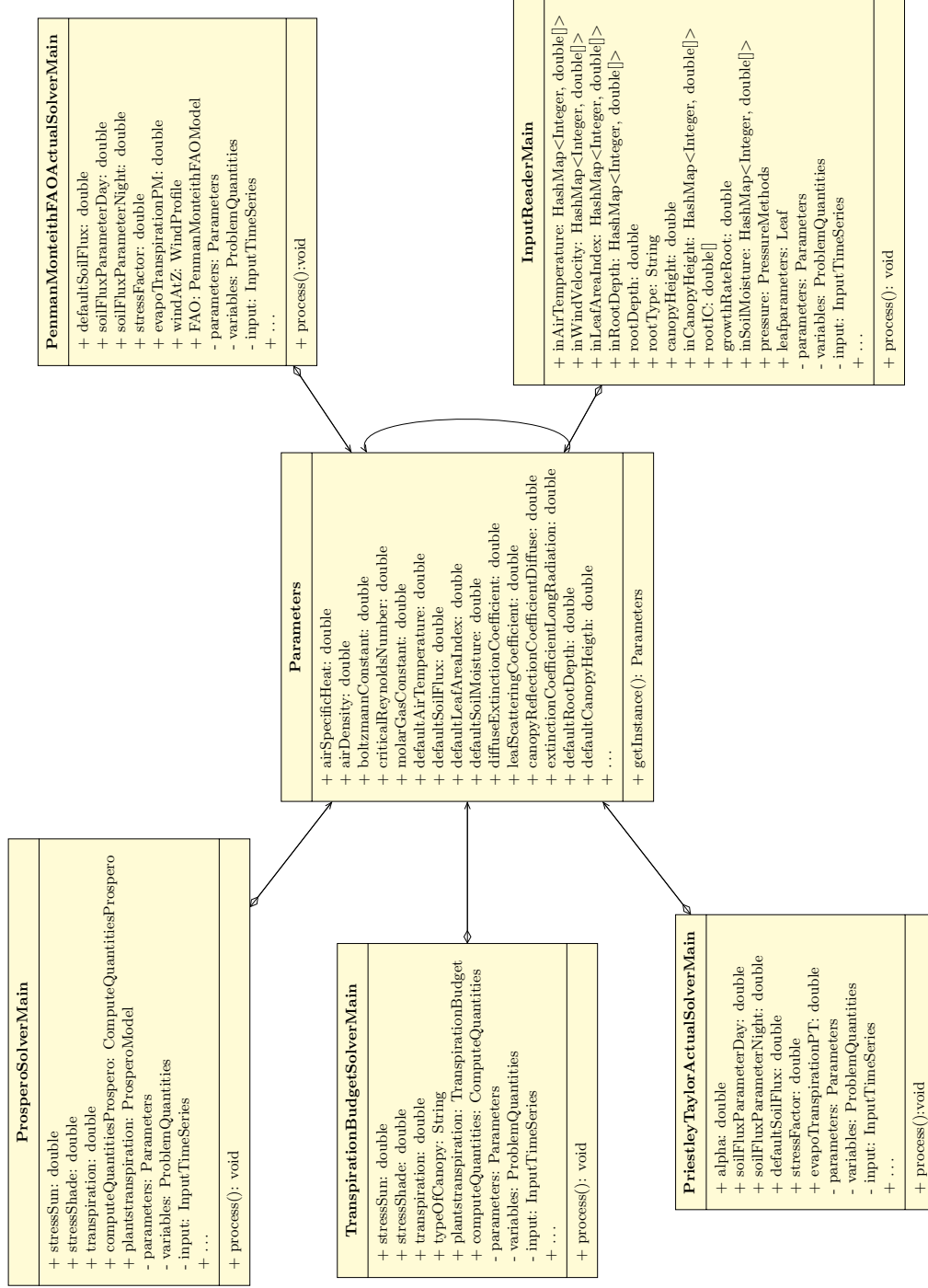


**Figure 5.** UML class diagram for the `Parameters` class showing the relation of aggregation and association with the ET models solvers and the input reader class.

320 of soil evaporation. Conversely, soil evaporation can reduce the available moisture for plant roots, impacting their ability to transpire effectively. This dynamic coupling shapes the moisture profile within the soil, significantly changing the overall water availability for the soil and vegetation and for the entire hydrological cycle.

C8-C29 The GEOET system incorporates three evapotranspiration models, as illustrated in Figure 6. In the following the formulas that implement them are reported for readers' convenience. First it comes the Priestley-Taylor one (Priestley and Taylor, 1972), secondly the Penman-FAO (Penman and Keen, 1948) and lastly the Prospero model (Bottazzi, 2020; Bottazzi et al., 2021). As described in Appendix A, Prospero solves the stationary energy budget coupled with water vapor transport and sensible heat transport using a zeroth-order approximation, incorporating information derived from the Clausius-Clapeyron equation. A comprehensive step-by-step derivation of the solution method is presented in D'Amato and Rigon (2025), which also addresses its current limitations and discusses potential enhancements. While the envisioned improvements are not yet implemented in the current GEOSPACE design, the software architecture has been carefully structured to accommodate future implementation of these and others advanced features.

### The Priestley-Taylor $E_T$ estimator

The GEOET system incorporates four evapotranspiration models, as illustrated in Figure 6. Starting with the simplest model, i.e., the widely used The Priestley-Taylor model component (PT) (Priestley and Taylor, 1972), which is based on the formula:

$$335 \quad ET_{PT} = \alpha \frac{\Delta}{(\Delta + \gamma)} (R_n - G) \quad (3)$$

where:  $\alpha$  is an empirical coefficient relating actual evaporation to equilibrium evaporation,  $\Delta$  is the slope of the saturation vapor pressure and air temperature curve [ $\text{kPa } ^\circ\text{C}^{-1}$ ],  $\gamma$  is the psychrometric constant [ $\text{kPa } ^\circ\text{C}^{-1}$ ],  $R_n$  is the net radiation [ $\text{W m}^{-2}$ ] and  $G$  is the ground heat flux [ $\text{W m}^{-2}$ ].

The implementation of this formula is relatively straightforward, although the radiation term requires a more detailed and careful evaluation. Further information about this equation can be found in Appendices A.

### The Penman-Monteith FAO estimator

The second model at present implemented is the Penman-Monteith FAO approximation (PM) (Penman and Keen, 1948), an adaptation of the Penman-Monteith model, as outlined in the following equation (G., 1986):

$$ET_0 = \frac{1}{\lambda} \frac{0.408\Delta(R_n - G) + \gamma \frac{900}{T+273} u_2 \delta_a}{\Delta + \gamma(1 + 0.34u_2)} \quad (4)$$

345 where,  $ET_0$  is the reference evapotranspiration [ $\text{mm day}^{-1}$ ],  $R_n$  is the net radiation at the crop surface [ $\text{MJ m}^{-2} \text{day}^{-1}$ ],  $G$  is the soil heat flux density [ $\text{MJ m}^{-2} \text{day}^{-1}$ ],  $T$  is the mean daily air temperature at 2 m height [ $^\circ\text{C}$ ],  $u_2$  is the wind speed at 2 m height [ $\text{m s}^{-1}$ ],  $e_s$  is the saturation vapour pressure also known as vapor pressure at the dew point [ $\text{kPa}$ ],  $e_a$  [ $\text{kPa}$ ] is the actual vapour pressure,  $\delta_a := (e_s - e_a)$  [ $\text{kPa}$ ] is the saturation vapour pressure deficit,  $\Delta$  [ $\text{kPa } ^\circ\text{C}^{-1}$ ] is the derivative of the Clausius-Clapeyron formula.

350 In terms of computational complexity, these models are relatively straightforward. Both PT and PM are equipped with dedicated packages housing their respective core Java classes for solving the equations, `PriestleyTaylorModel.java` and `PMFAOModel.java`. Additionally, each package includes various 'Solver' classes designed to invoke methods from the main model class, enabling the computation of solutions that account for environmental inputs and stress factors.

Specifically, to ensure that users do not input more information than necessary or provide data unrelated to their chosen method, we differentiate between solvers for calculating potential evapotranspiration (without stresses) and actual evapotranspiration (with the possibility to select among the various type of stresses).

### The Prospero Model

The Prospero model (Bottazzi, 2020; Bottazzi et al., 2021), is a physically based approach for calculating transpiration as detailed in D'Amato and Rigon (2025). The transpiration,  $E_l$ , is considered for the sunlit and shaded fractions of the canopy while the soil evaporation,  $E_s$ , is estimated using the residual radiation hitting the soil.  $E_s$ , at present, is determined according the 360 FAO Penman–Monteith model, i.e.  $E_s = ET_0$ . Meanwhile,  $E_l$  is computed using Prospero model that implements a modified version of the Schymanski and Or (SO) model (Schymanski and Or, 2017), which has been upscaled to address canopy-level transpiration and ensure mass conservation during periods of water stress.

As described in Appendix A, SO solves the stationary energy budget coupled with the water vapor transport and sensible 365 heat transport in a zeroth-order approximation, with the help of information derived from the Clausius–Clapeyron equation. Furthermore, This model returns, not only a  $E_l$  estimate but also the sensible heat  $H$  and vapor pressure gap  $e_\Delta$ , besides the temperature of the leaves,  $T_l$ . The latter variable is the key for obtaining the others, as below:

$$T_l = \frac{R_n + a_{sH} A_{tr} \epsilon_l \sigma T_a^4 + c_H(a_{sH}, A_{tr}) \cdot T_a + c_E(a_{sE}, A_{tr}, g_s) \cdot (\Delta \cdot T_a + \delta_a)}{c_H(a_{sH}, A_{tr}) + c_E(a_{sE}, A_{tr}, g_s) \Delta + a_{sH} A_{tr} \epsilon_l \sigma T^3} \quad (5)$$

where:  $R_n$  is the the net radiation,  $a_{sH}$  is the sides of surface exchanging sensible heat and longwave radiation, equal to 1 370 for single-layer exchange, 2 for two-layer exchange such as leaves[-],  $A_{tr}$  is the transpiring surface for unit of ground surface [-],  $\epsilon_l$  [-] is the leaves emissivity,  $\sigma = 1.6710^{-8}$  [Wm<sup>-2</sup>K<sup>-4</sup>] is the Stefan-Boltzmann constant,  $a_{sE}$  represents the sides of surface exchanging latent heat, equal to 1 for hypostomatous, and 2 for amphistomatous [-],  $g_s$  is the stomatal conductance [ms<sup>-1</sup>],  $\delta_a = P_{ws}$  and  $P_w$  are the saturation water vapour pressure and the water vapour pressure, respectively,  $c_E$  is the total conductance for water vapor evapotranspiration transport [ms<sup>-1</sup>] and  $c_H$  is the total conductance for the sensible heat transport 375 [ms<sup>-1</sup>].

It is assumed that the right-hand-side terms in Equation 5 are all known. Furthermore, the water pressure gap is estimated as follows:

$$e_\Delta := e_s - e_l = \Delta(T_l - T_a) + \delta_a \quad (6)$$

The transpiration is calculated as:

$$380 \quad E_l = c_E(a_{sE}, A_{tr}) e_\Delta; \quad (7)$$

Finally, the sensible heat is computed as:

$$H_l = c_H (a_{sH}, A_{tr}) (T_l - T_a) \quad (8)$$

For further information on these formulas or solutions, please refer to Bottazzi (2020), Bottazzi et al. (2021) or D'Amato and Rigon (2025).

#### 385 4.1 The GEOET informatics organization

The evapotranspiration component, GEOET, developed as part of this paper, is based on its precursor, GEOframe-ETP model (Bottazzi, 2020; Bottazzi et al., 2021) whose original source code is available at <https://github.com/geoframecomponents/ETP>. Both GEOframe-ETP and GEOET simulate the evapotranspiration according to different evapotranspiration models: the Priestley-Taylor model (Priestley and Taylor, 1972), the Penman-Monteith FAO model (Allen et al., 1998), and the GEOframe-Prospero model (Bottazzi, 2020; Bottazzi et al., 2021). But, in moving from one software to the other, the refactoring of the existing codes was substantial both at design level and algorithmic level, as you can see in the box diagrams of Figure 6. The reorganization and the re-engineering of the software were essential to allow the use of multiple options of evapotranspiration physics, to introduce a separate component for calculating the stress factor, making possible to apply them to all evapotranspiration models, and facilitating the connection of any of the ET components with other model components and particularly enabling its linkage with WHETGEO.

The new version of the code thus allows the physical processes of evapotranspiration to be analysed individually and also in conjunction with the infiltration process. To obtain this, as shown in Figure 6, all the evapotranspiration models were separated into packages of classes with specific tasks. Furthermore, depending on the model's complexity, each package is hierarchically organized into additional packages and classes. Each class is designed to perform a singular task and strives to be as self-contained as possible. This design not only ensures that each class operates independently but also shields the user from the need to provide inputs or information unrelated to the specific model they are utilizing.

The new packages include:

- `geoet.data` is the package responsible for managing the data and variables of all the ET models. The data are encapsulated in singleton static classes that are simultaneously available to all the other classes of estimating ET, as previously described for the data classes functional to WHETGEO.
- `geoet.inout` package was crafted to facilitate the management of model inputs and outputs. As the model's evolution aligns with contemporary trends to separate model-agnostic data from the models themselves. This software structure, in fact, allows for the incorporation of diverse data ingestion and extraction methodologies and is pivotal in harnessing novel data handling advancements as they emerge.

410 Besides the packages dedicated to ancillary shared task, packages were dedicated to contain the various algorithms for each of the evapotranspiration estimation model used:

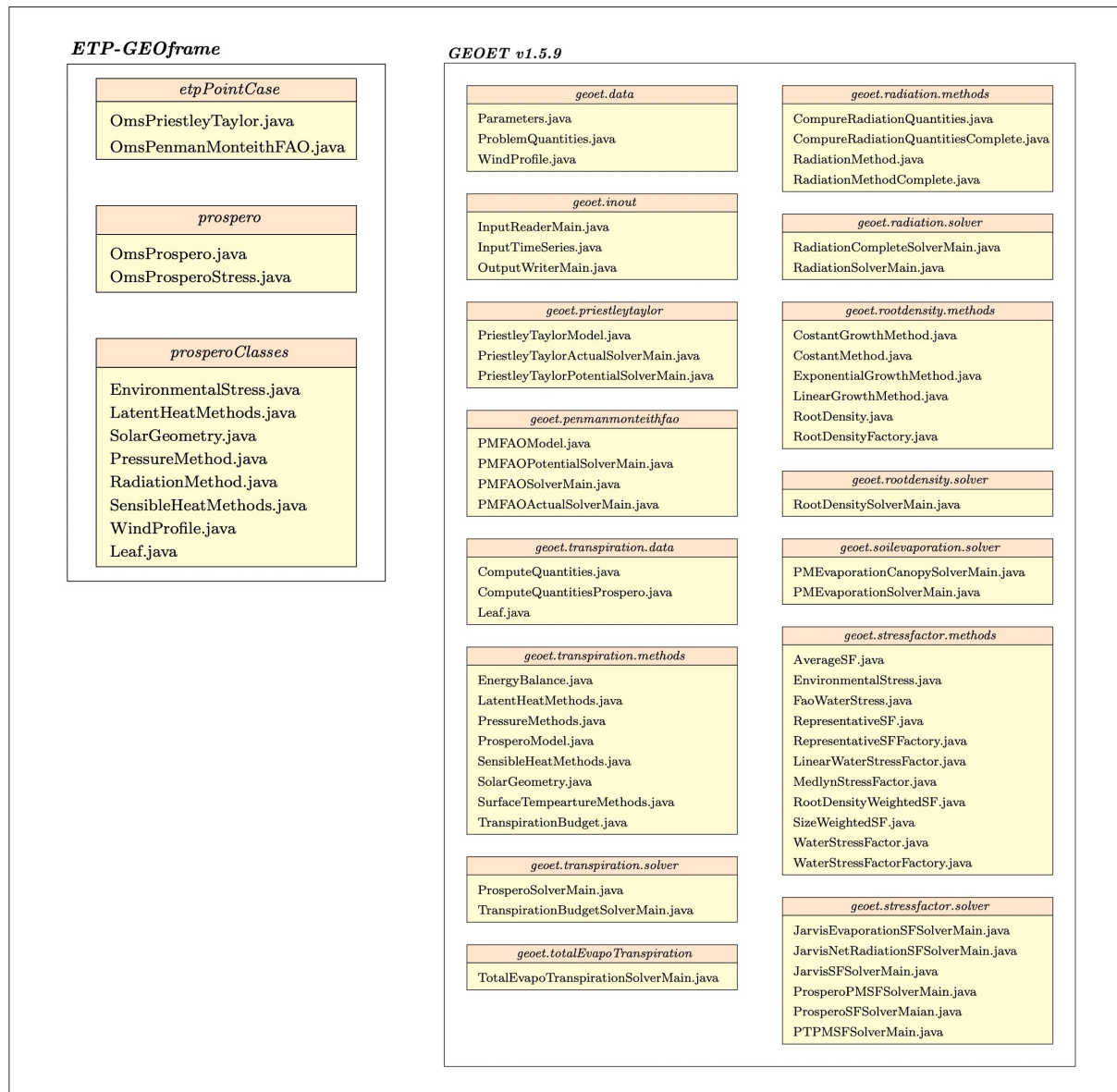


**Figure 6.** The GEOframe ET original packages, constituting ETP-GEOframe, (Bottazzi, 2020) (on the left) and the new packages (on the right) containing in GEOET. This refactoring was necessary to accommodate multiple options for estimating the water stress factor, incorporate a more sophisticated radiation budget, and integrate a model for root functioning.

- Priestley-Taylor formulation (Priestley and Taylor, 1972) of ET is implemented in the `geoet.priestleytaylor` package;
- Penman-Monteith FAO model is implemented in the `geoet.penmanmonteithfao` package;
- 415 – Prospero model is more conceptually and computationally complex than the other two models and, as can be seen in Figure 6, is split into various packages and the relative packages are named `geoet.transpiration.*`.

A specialized package has been developed exclusively for estimating the soil evaporation, designated as `geoet.soil-evaporation.solver`. In this phase, the computation of soil evaporation employs the Penman-Monteith method. However, the software's architecture is designed to facilitate effortless integration and development of novel techniques based on the theory supported by the work by Lehmann et al. (2014).  
420

Enclosed within the `geoet.radiation.*` packages lie the procedures inherited from the earlier ETP-GEOframe version, alongside the methodologies introduced in this study, expounded in the Supplement, which build upon the parameterizations of the processes delineated in de Pury and Farquhar (1997) and Ryu et al. (2011).

#### 4.1.1 How to add a new model?

425 **C8** A primary objective in the software engineering of the GEOSPACE system was to enable feature expansion through class addition rather than code modification, adhering to the open-closed principle of object-oriented design. By following the OOP and generic programming principles of GEOSPACE-1D, integrating a new model component, either a solver or a new stress function into the existing codebase becomes, in fact, straightforward. To illustrate this feature that actually applied to any part of GEOSPACE, consider the introduction of a new stress model. To incorporate it, a concrete class is created  
430 within the `geoet.stressfactor.methods` package, such as `HydroDemo.java`, where the numerical equation for the new method is defined. Furthermore, a solver class is developed within the `geoet.stressfactor.solver` package, for instance, `HydroDemoSolverMain.java`. This class solves the equation by directly invoking methods from the concrete classes. This integration is achieved through addition, requiring no modifications to previously written code.

The newly created class, `HydroDemo.java`, extends the existing abstract class, `WaterStressFactor.java` (see  
435 Section 5.4). This new class provides the implementation of the concrete method defined in the abstract class and inherits all of its characteristics. Finally we update the file `WaterStressFactorFactory.java` with the string that users must enter in the model executable to specify the new method they wish to use, namely "HydroDemo".

## 5 About the stress factors models and their deployment

As highlighted in the Supplement, the modeling of stomatal conductance, often referred to as "vegetation stress factor", stands  
440 as a central subject of debate within the scientific literature. This contentious issue has spurred the emergence of multiple theoretical frameworks, each trying to provide a comprehensive understanding of this intricate physiological process (Daly et al., 2004).

It is essential to have a computer modelling framework that facilitates the integration of emerging theories without compromising the integrity of the current code. This capability of GEOSPACE-1D ensures that it can adapt in harmony with new  
445 research advancements, thereby enhancing the resilience and relevance of its computational framework.

The scientific literature unfolds two primary families of parameterizations governing leaf conductance (Yu et al., 2017), the Jarvis model (Jarvis et al., 1976) and the Ball-Berry one (Dewar, 2002) and it is pivotal to create an informatics infrastructure capable of implementing both these formulations. To achieve this, we constructed an adaptable set of packages:  
`geoet.stressfactor.*`.

450 The forthcoming implementation we are detailing must seamlessly function with both the GEOET model independently and when integrated with GEOSPACE-1D. In each scenario, it should have the flexibility to accommodate different stress factor models. This abstraction is essential as stress factor data pertaining to each control volume is not only crucial for GEOET but also necessary for BrokerGEO and WHETGEO within the GEOSPACE-1D framework.

So far, two stress parameterizations were implemented, the so called Jarvis model (Jarvis et al., 1976; Macfarlane et al.,  
455 2004; White et al., 1999) and the Medlyn stomatal conductance model (Medlyn et al., 2011).

## 5.1 The Jarvis Model for stresses

As described in the Supplement, the Jarvis model implemented in GEOET follows the version of the model proposed by White et al. (1999) and by Macfarlane et al. (2004), where the stomatal conductance is equal to:

$$g_s = g_{s,max} \cdot f_R(R_{PAR}) \cdot f_T(T_a) \cdot f_\delta(\delta_a) \cdot f_\psi(\psi_l) \quad (9)$$

460 where we have stresses for the photosynthetically active radiation (PAR)  $f_R(R_{PAR})$ , the air temperature  $f_T(T_a)$  and the water pressure deficit  $f_\delta(\delta_a)$ . All the information about the  $f$  functions implemented are detailed in the dedicated Supplement and are implemented in the `EnvironmentalStress.java` class.

As regards the water stress, despite the wealth of literature, in a considerable number of soil-plant model, water availability directly depends on  $\theta$  (Verhoef and Egea, 2014a) rather than on  $\psi$ . Following what was done in the precursor GEOframe-ETP  
465 model (Bottazzi, 2020), we maintained the FAO water stress factor  $K_s$  (Appendix A) and a new formulation was added as function  $f_\theta(\theta)$ , the "Fraction of Transpirable Soil Water" (FTSW), to be used in the Jarvis model (Eq. 9). The formula itself is a representation of the relationship between soil moisture content ( $\theta$ ), wilting point ( $\theta_{WP}$ ), and field capacity ( $\theta_{FC}$ ), and it is commonly used to assess plant water stress and to make decisions related to irrigation management and water conservation. The java class involved in the computation of the FTSW is the `LinearWaterStressFactor.java` class and computes  
470 the water stress factor in each control volume of the grid computational soil according to the following:

$$g_{w,i} = \frac{\theta_i - \theta_{WP,i}}{\theta_{FC,i} - \theta_{WP,i}} \quad (10)$$

where:

- $g_{w,i}$  is the water stress factor in the  $i$ -th control volume;

- $\theta_i$  represents the current soil water content in the  $i$ -th control volume;
- 475 –  $\theta_{WP,i}$  is the wilting point of the  $i$ -th control volume of the soil, which is the moisture level at which plants can no longer extract water from the soil effectively, leading to wilting;
- $\theta_{FC,i}$  represents the field capacity of the  $i$ -th control volume of the soil, which is the maximum amount of water the soil can hold against the force of gravity.

The  $\theta_i$  value derived from the WHETGEO model, likewise, the parameters  $\theta_{WP,i}$  and  $\theta_{FC,i}$  are customized for each control  
480 volume, as it is the user's choice to discretize the soil column and determine the number of layers and associated parameter values. Consequently, the values of  $\theta_{WP,i}$  and  $\theta_{FC,i}$  are specific to each individual soil layer and, by extension, to all the control volumes containing them.

## 5.2 The Medlyn model for stresses

The Medlyn model (Medlyn et al., 2011) is part of the Ball-Berry-Leuning (BBL) family of models (Ball et al., 1987; Leuning,  
485 1990; Dewar, 2002) and it has been modified in various ways since the original paper. For instance, in Dewar (2002) the form given to it is:

$$g_B = g_0 + g_1 \frac{A_n}{(C_s - \Gamma) \left(1 + \frac{\delta_a}{e_0}\right)} \quad (11)$$

where:  $g_B$  is the Ball-Berry-Leuning conductance;  $g_0$  is the value of  $g_B$  at the light compensation point;  $g_1$  and  $e_0$  are  
490 empirical coefficients;  $A_n$  is the net leaf  $CO_2$  assimilation rate;  $C_s$  is the  $CO_2$  concentration at the leaf surface;  $\Gamma$  is the  $CO_2$  concentration at the compensation point; and finally  $\delta_a$  is the water vapor pressure deficit.

An interesting form of the BBL was obtained in Medlyn et al. (2011), under the hypothesis of optimal photosynthesis theory, which is:

$$g_B = 1.6 \left(1 + \frac{g_1}{\sqrt{\delta_a}}\right) \frac{A_n}{C_s} \quad (12)$$

The equation (12) has been integrated into the GEOSPACE-1D framework simply by adding a class:

495 – `MedlynStressFactor.java`

and it is fully functional when a time series of net carbon assimilation is provided as input. Its scope actually, is to be a placeholder for a future OMS3 component dedicated to computing net carbon assimilation within the GEOSPACE-1D.

## 5.3 Estimating the global stress on the basis of local stresses

Given the discretization of soil into multiple layers within GEOSPACE-1D, it becomes imperative to establish a method for  
500 distributing total stress estimates based on local stresses and reciprocally allocating transpiration demands across these soil layers. The mechanism through which soil moisture is transported into plants, thereby facilitating  $E_1$  is primarily via the roots

(Carminati and Javaux, 2020), hence, despite its simplicity, the introduction of a root functioning model is essential. Within GEOSPACE-1D, root models are integrated into GEOET, through:

- `geoet.rootdensity.methods` package;
- 505 - `geoet.rootdensity.solver` package.

Eventually, at this point, the information derived by the root models can be used to estimate the total stress acting on the plants. GEOET implements three ways to estimate the global stress C31 called: **Average Water Stress factor, Size Weighted Stress factor, Root Density Weighted Water Stress Factor**, which are briefly described below.

- **Average Water Stress Factor** ~~This method~~ is implemented in the `AverageSF.java` class, according to which the representative water stress factor value at the  $n$ -th instant,  $G_w$ , is given by the arithmetic mean of the stress values characterising the soil column:
- 510

$$G_w = \frac{\sum_{i=1}^N g_{w,i}}{N} \quad (13)$$

where  $N$  is the total number of control volumes affected by the roots.

- **Size Weighted Water Stress Factor** ~~This method~~ is implemented in the `SizeWeightedSF.java` class, according to which the representative water stress factor value at the  $n$ -th instant,  $G_w$ , is given by the weighted average of the water stress values characterising the soil column as a function of the size  $dx$  of the control volumes affected by the roots:
- 515

$$G_w = \frac{\sum_{i=1}^N g_{w,i} \cdot dx_i}{\sum_{i=1}^N dx_i} = \frac{\sum_{i=1}^N g_{w,i} \cdot dx_i}{\eta_R} \quad (14)$$

It is specified that the sum of the size  $dx_i$  of the control volumes affected by the root system coincides with the depth  $\eta_R$  of the roots themselves.

- **Root Density Weighted Water Stress Factor** ~~This method~~ is implemented in the `RootDensityWeightedSF.java` class, according to which the representative water stress factor value at the  $n$ -th instant,  $G_w$ , is given by the weighted average of the water stress values characterising the soil column as a function of the root density  $\rho_{R,i}$  of the control volumes affected by the roots:
- 520

$$G_w = \frac{\sum_{i=1}^N g_{w,i} \cdot \rho_{R,i}}{\sum_{i=1}^N \rho_{R,i}} = \frac{\sum_{i=1}^N g_{w,i} \cdot \rho_{R,i}}{\rho_{Root}} \quad (15)$$

- In this case the sum of the root density in each control volumes  $\rho_{R,i}$  affected by the root system coincides with the total root density in the root zone  $\rho_{Root}$ .
- 525

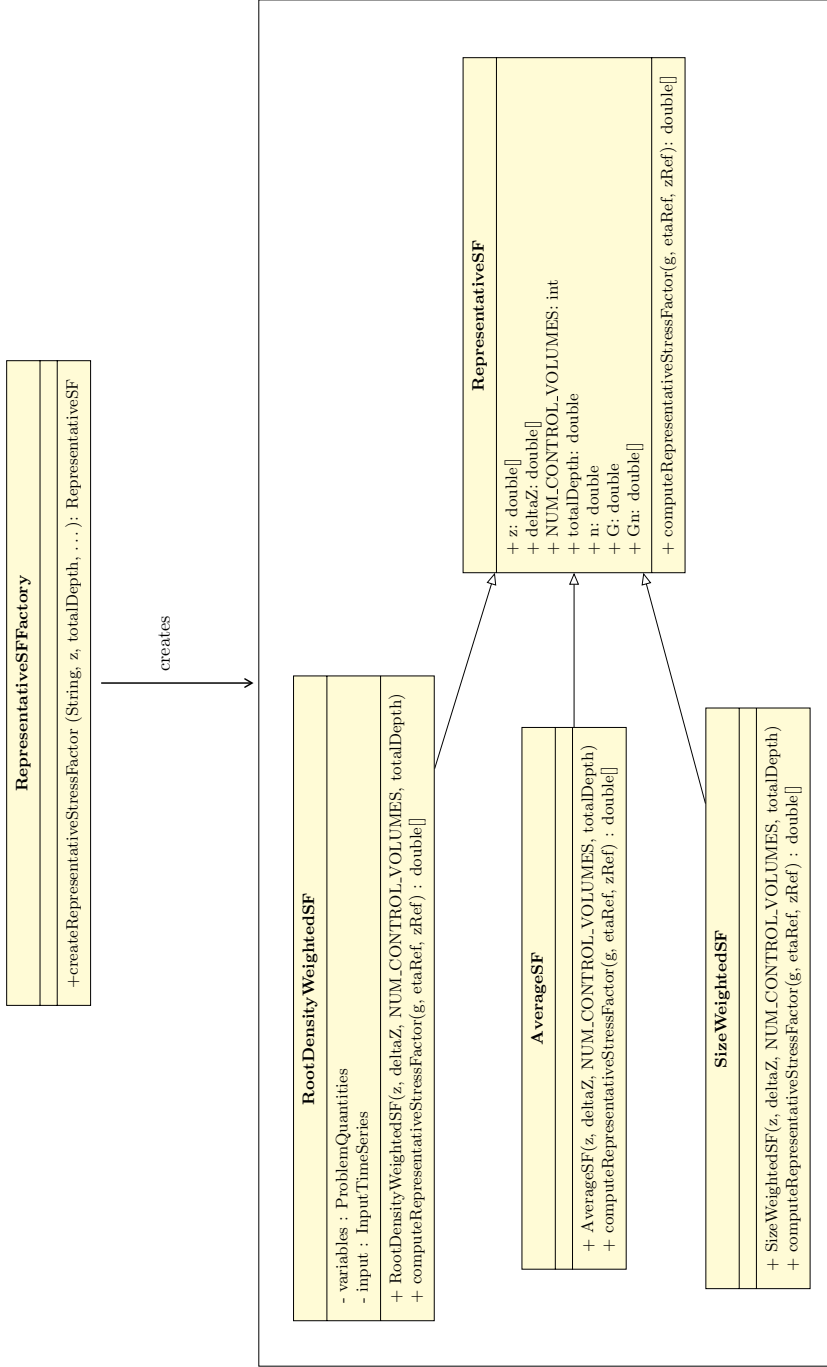


**Figure 7.** UML class diagram for the Java Simple Factory applied for the choice of the representative water stress factor computation model. The `RepresentativeSF` class defines the interface that is implemented by the concrete classes `RootDensityWeightedSF`, `AverageSF` and `SizeWeightedSF`.

## 5.4 Informatics: factory pattern for stress estimator

The multiplicity of parameterizations in the literature for the calculation of the stomatal conductance, as well as the numerous formulations that can be used for the computation of a representative stress factor value, pose precisely the problem of how to implement a structure that is flexible to current and future changes. To do this, we relied on the potential of the design, i.e., the Simple Factory Pattern (Gamma et al., 1995). If we consider the case of the computation of the representative water stress factor value, we practically need different subclasses that implement several methods with the possibility of the user to choose one of these classes, and also add new method in the future. Indeed, employing the Simple Factory Pattern (Freeman et al., 2008; Gamma et al., 1995) enables the encapsulation of object creation logic within the factory class.

As shown in Figure 7, `RepresentativeSF` class is an abstract class and three java classes that implement the concrete methods to compute the representative water stress factor:

- `RootDensityWeightedSF`;
- `AverageSF`;
- `SizeWeightedSF`.

A closer inspection of Figure 7 reveals that the `RepresentativeSFFactory` class accomplishes the task of implementing one of the concrete classes. In particular the `RepresentativeSFFactory` class is responsible for creating instances of `RepresentativeSF` or its subclasses based on a specified type provided as input. The `RepresentativeSFFactory` class is connected to the classes `RepresentativeSF` and its possible subclasses through the `createRepresentativeStressFactor` method. The factory creates instances of `RepresentativeSF` or its subclasses based on the specified type and returns them as output.

In the context of computing water stress within each control volume, an abstract and factory class framework were developed, like the one just described, using the java classes `WaterStressFactor` and `WaterStressFactorFactory`. This architecture was designed with the foresight of accommodating novel formulations.

## 6 BrokerGEO actions and packages

It is important to note that the ET (or T) flux drawn from the soil from each control volume estimated by GEOET, is subject to a water stress which depends on the the existing water content estimated by WHETGEO, establishing a feedback between the two software components. To implement the feedback, BrokerGEO distributes the evaporative demand among the soil control volumes. The three methods implemented below mirror the methods used to obtain the global water stress factor in GEOET for any time step:

*AverageWaterWeightedMethod*

$$ET_{ref,i} = \frac{g_{w,i}}{\sum_{i=1}^N g_{w,i}} ET_{ref} = \frac{g_{w,i}}{N G_w} ET_{ref} \quad (16)$$

### *SizeWaterWeightedMethod*

$$ET_{ref,i} = \frac{g_{w,i} \cdot dx_i}{\sum_{i=1}^N g_{w,i} \cdot dx_i} ET_{ref} = \frac{g_{w,i} \cdot dx_i}{G_w \eta_R} ET_{ref} \quad (17)$$

### *RootWaterWeightedMethod*

560 
$$ET_{ref,i} = \frac{g_{w,i} \cdot \rho_{R,i}}{\sum_{i=1}^N g_{w,i} \cdot \rho_{R,i}} ET_{ref} \quad (18)$$

where  $ET_{ref}$  is the reference flux at the  $n$ -th instant,  $ET_{ref,i}$  is the splitted flux at the  $n$ -th instant in each  $i$ -th control volumes,  $N$  is the total number of control volumes affected by the roots,  $dx$  is the size of the control volumes,  $\eta_{ref}$  is the depth at which we want to divide the flow, which can be the depth of the roots or the depth of the soil layer that is considered for evaporation. Finally  $\rho_{R,i}$  is the root density in each control volumes and  $\rho_{Root}$  is the total root density. The  $g_{w,i}$  are the water stress factor in the  $i$ -th control volume at the  $n$ -th instant,  $G_w$  is the representative water stress factor and the other symbols used have the meanings mentioned above.

565

## 6.1 BrokerGEO informatics

BrokerGEO is an independent OMS3 component used in GEOSPACE-1D to connect WHETGEO-1D to the four different evapotranspiration models of GEOET. The BrokerGEO 1.3.9 version is mainly composed of three packages shown in Figure 8:

570

- brokergeo.data
- brokergeo.solver
- brokergeo.methods

The `brokergeo.data` package assumes the role of overseeing the input data and variables associated with the models. It leverages on two classes, namely `ProblemQuantities` and `InputData` for input management. These classes are subsequently linked to the classes responsible for computing the partitioned evapotranspiration within each control volume, which are within the `brokergeo.solver` package. The `solver` packages contains classes that are designed to invoke methods from the classes in `brokergeo.methods`, enabling the computation of solutions.

575

In the UML diagram depicted in Figure 9, the package comprises two key solver classes: firstly, `ETsBrokerOneGenericFluxSolverMain`, which is tailored for computing only the split evapotranspiration (ETs). This approach aligns with the prevalent practices in evapotranspiration modeling literature, where most models estimate the comprehensive evapotranspirative flux, encompassing both vegetation transpiration and bare soil evaporation. However, models like Prospero and TranspirationBudget are dedicated exclusively to transpiration computation. Secondly, `ETsBrokerTwoFluxesSolverMain` is specifically designed to calculate the split transpiration ( $E_1$ ) and split soil evaporation ( $E_s$ ) as distinct components.

580

### *BrokerGEO v1.3.9*

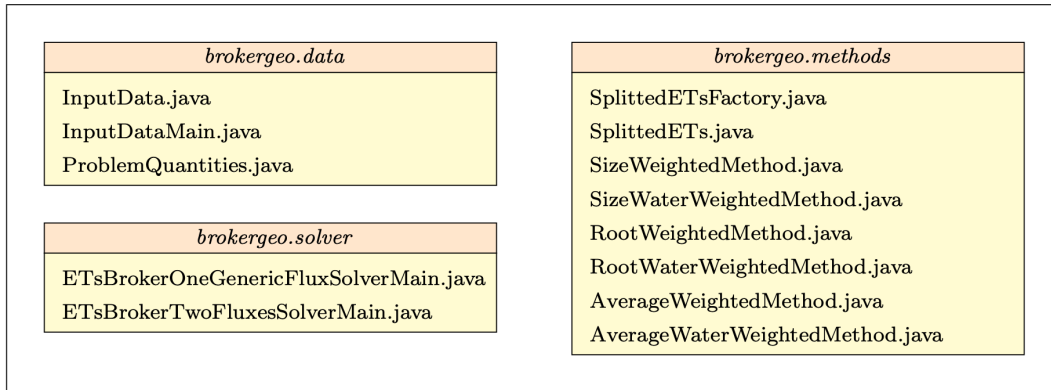


**Figure 8.** IT software structure of BrokerGEO v1.3.9: packages and classes.

585 Upon a more detailed examination of Figure 9, it becomes apparent that the connection between the solver classes, specifically `ETsBrokerOneGenericFluxSolverMain` and `ETsBrokerTwoFluxesSolverMain`, and the two classes `ProblemQuantities` and `InputData` can be characterized as a hybrid of both "association" and "aggregation."

At the bottom of the programming chain, three classes are responsible for implementing the three equations (16, 17, 18): `AverageWaterWeightedMethod.java`, `SizeWaterWeightedMethod.java` and `RootWaterWeighted-`  
590 `Method.java`. Any other possible partition formula can be implemented as well by simply adding a class in the method package.

## **6.2 BrokerGEO Factory Pattern**

Given that multiple methods for partitioning evapotranspiration (ET) can be employed, with the potential for introduction of new methods in the future, the most adaptable design choice for the IT architecture of BrokerGEO was the Simple Factory  
595 Pattern (Gamma et al., 1995).

As shown in Figure 10, `SplitterETs` class is the abstract class and it contains only the abstract method `computeStressedETs`. Therefore, we have six possible alternatives that implement a concrete method to compute the splitted flux:

- `AverageWaterWeightedMethod`,
- `AverageWeightedMethod`,
- 600 - `RootWaterWeightedMethod`,
- `RootWeightedMethod`,
- `SizeWaterWeightedMethod`,

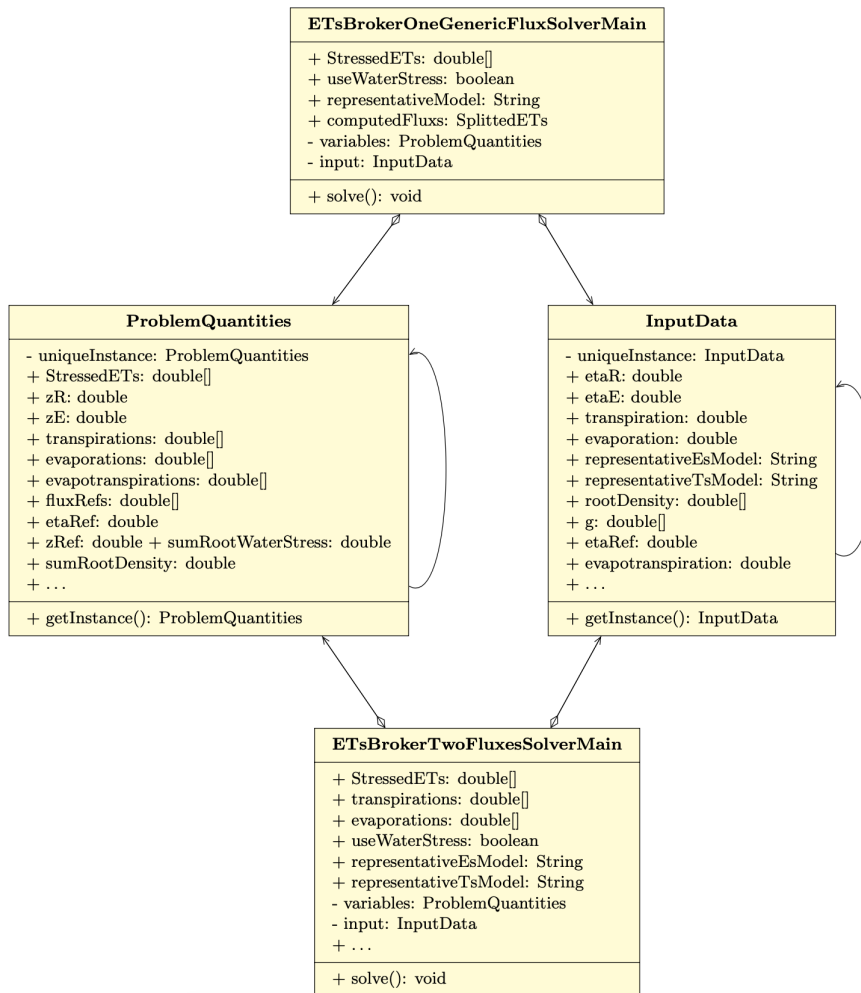


**Figure 9.** UML class diagram for the ETsBrokerOneGenericFluxSolverMain class and ETsBrokerTwoFluxesSolverMain class. The classes compute the splitted evapotranspiration directly calling the methods of the concrete classes through the Simple Factory Pattern shown in Figure 10. The graph points out the relation of "aggregation" and "association" between the solver classes and ProblemQuantities InputData classes.

- SizeWeightedMethod.

The connection between the *SplitterETsFactory* class and the *SplitterETs* class is established through the *createEvapoTran-*  
605 *spirations* method. This method enables the factory to produce instances of *SplitterETs* and its subclasses based on the specified type string that the user may specify as input to choose which model to use and the corresponding method is returned.

Since BrokerGEO operates as an autonomous OMS3 component, all the implemented numerical methods are capable of partitioning a reference flux. This reference flux may represent simple evaporation, transpiration, or the entire evapotranspiration flux.

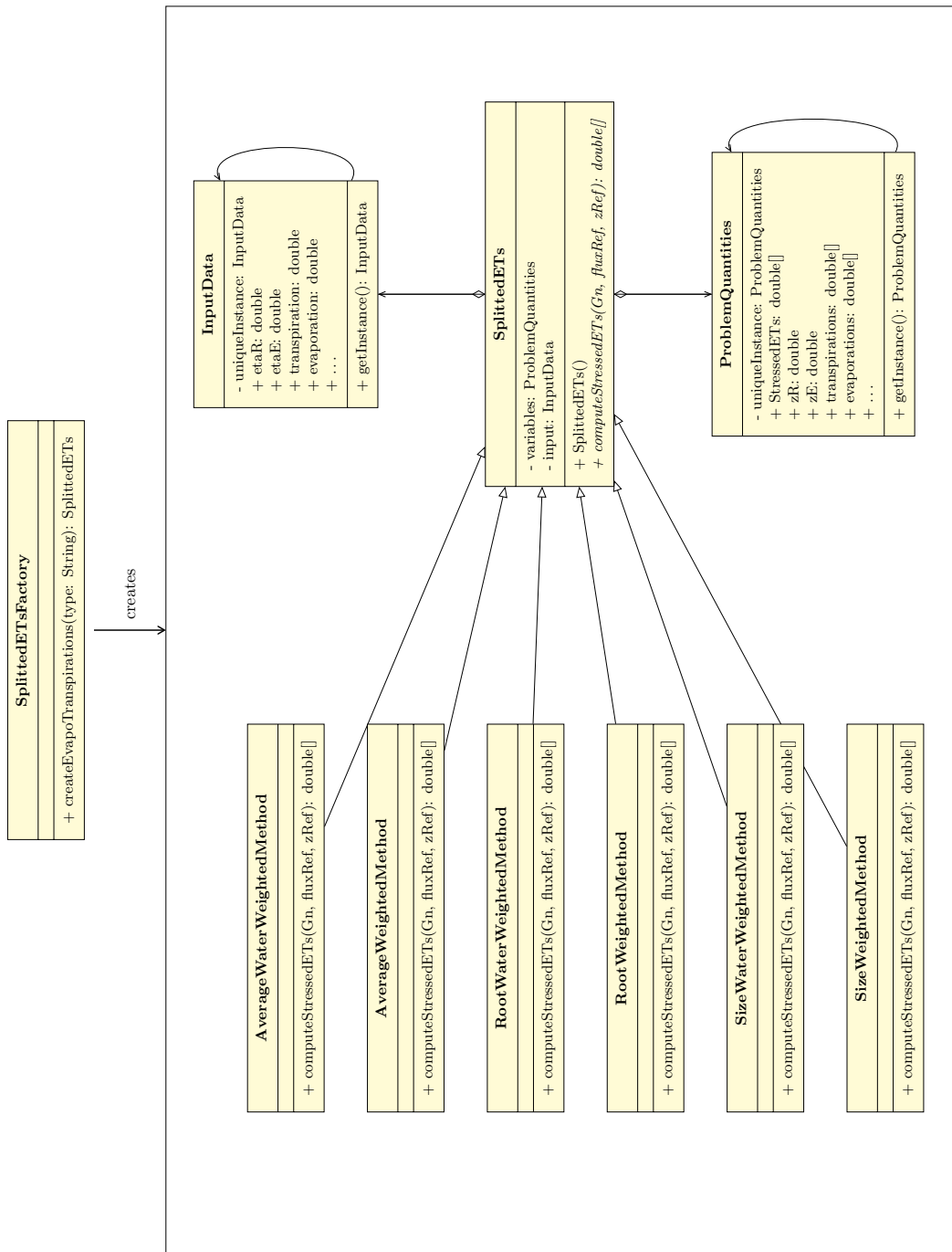


**Figure 10.** UML class diagram for the Java Simple Factory applied for the choice of the splitter evapotranspiration method. The SplittedETs class defines the interface that is implemented by the concrete classes AverageWaterWeightedMethod, AverageWeightedMethod, RootWaterWeightedMethod, RootWaterWeightedMethod, RootWeightedMethod, SizeWaterWeightedMethod and SizeWeightedMethod. The UML graph points out the relation of "aggregation" and "association" between the abstract class SplittedETs and ProblemQuantities and InputData classes.

To demonstrate the capabilities of the model, we present a two "virtual" simulations: the first called as "baseline simulation" (BSL) which simulates the coupled dynamics of infiltration and evapotranspiration, while the second one focuses only on the infiltration process. is described below with the scope to showcase the potential applications and capabilities of the coupled system of GEOSPACE-1D model and verify its correct functioning. C5-C32 The simulations are not intended to investigate a particular experimental setup, which would require a longer paper and open a topic better addressed in dedicated research. Instead, these simulations serve as a proof of concept, demonstrating that the system functions correctly without integration errors across all tested conditions. This represents only a small subset of the comprehensive simulations performed by the Authors to evaluate GEOSPACE's robustness. Water budget closure was verified for all simulations, with supporting documentation provided in the supplemental material. All the simulations are readily available in the supplemental material which contain a series of Jupyter notebooks which allow to re-execute them and inspect their results more deeply.

The BSL simulation was done by forcing the model with the input data of the two-month dataset from the "Spike II" experiment whose forcings are shown in Figure 11. A comprehensive description of the experiment is reported in Queloz et al. (2015), Benettin et al. (2019), Benettin et al. (2021a), Benettin et al. (2021b) and Nehemy et al. (2021).

The "Spike II" BSL can be described as a one-dimensional simulation of a homogeneous column of soil of 2.5 m depth with a plant of height of 3.5 m, i.e. a willow. The soil column was discretized with a uniform grid space of 250 control volumes and we carried on a hourly time-step simulation. The soil hydraulic properties are described with the Van Genuchten's model (Table 2), and most of them are taken from the work of Asadollahi et al. (2022). The initial condition is assumed to be hydrostatic with  $\psi = 0$  m at the bottom. The surface boundary condition is the rainfall and irrigation shown in Figure 11 (a). WHETGEO-1D (Tubini and Rigon, 2022) includes a surface water coupled model which allows the formation of surface ponding, and so the surface boundary condition may change from the Dirichlet type - prescribed water suction - to the Neumann type - prescribed flux - and vice-versa, according to the occurring process. At the bottom of the column, we prescribed a free drainage boundary condition with a gravity-driven transient.

For the evapotranspiration model, we utilized the GEOET-Prospero model, driven by the input data shown in Figure 11. Our analysis focused on a plant of height of 3.5 m, with leaf area index (LAI) linearly varying from 2.5 to 4 m at the beginning and end of the simulation, respectively. As root depth and density parameters we used the "Spike II" experiment measurements of the willow and they were kept constant throughout the simulation. Finally, among the Jarvis stress only the water stress is considered, excluding all environmental stresses and the representative water stress factor for transpiration  $G_{Tw}$  is computed with the root density weighted method. The representative water stress factor for evaporation  $G_{Ew}$  is calculated as the arithmetic mean of the stress values characterizing the depth of the evaporation layer, located 0.2 m from the soil surface. The partitioning of evaporation and transpiration between the control volumes is done by BrokerGEO using AverageWaterWeightedMethod for evaporation, and the RootWaterWeightedMethod for transpiration.

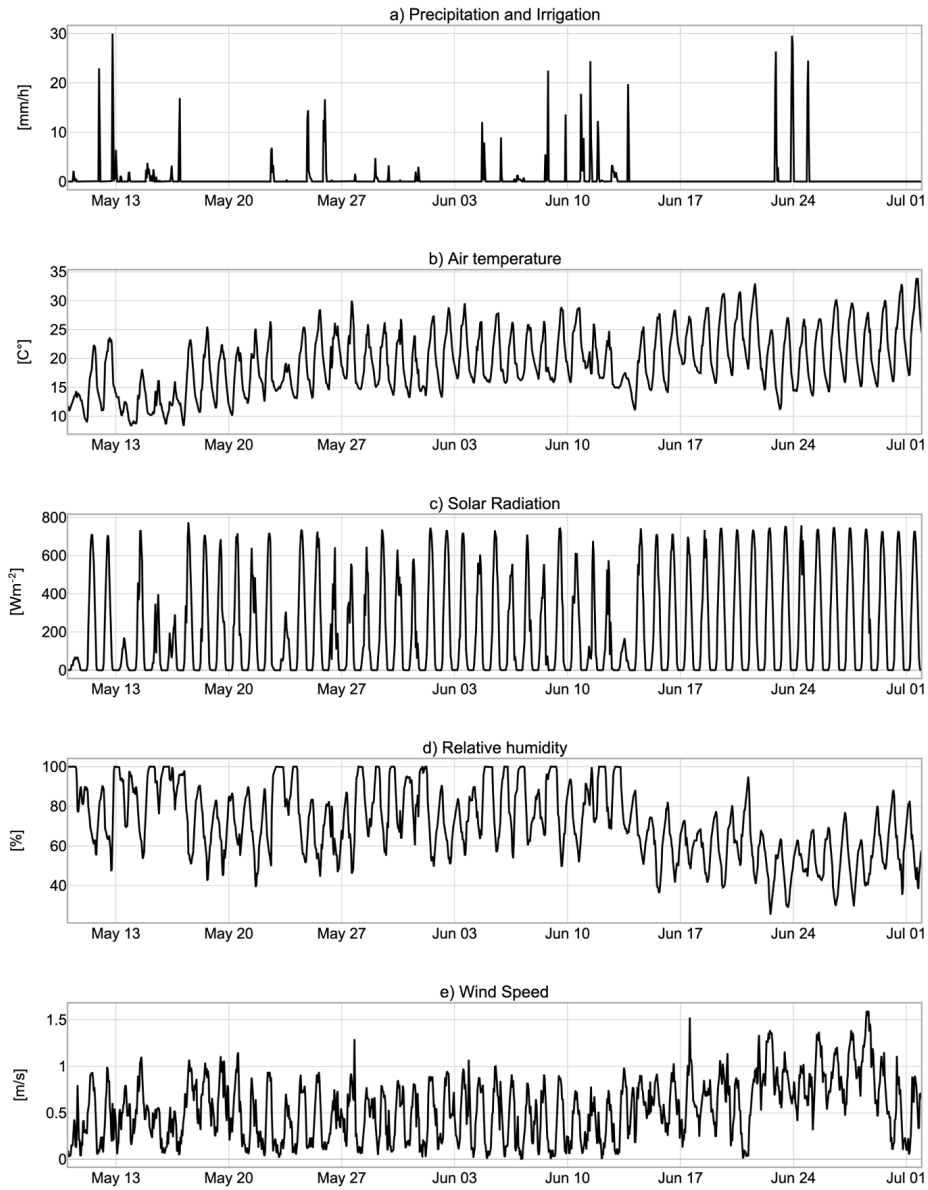


**Figure 11.** Timeseries of the dataset from "Spike II" experiment provided by the meteo station (MeteoMADD, MADD Technologies Sàrl, Switzerland). The data has been accurately aggregated on an hourly scale to be used as input of the simulation with GEOSPACE-1D model.

**Table 1.** Summary of the main settings for Baseline Simulation: This table presents key parameters and configurations utilized in the baseline simulation.

Soil column depth	2.5 m
n° Soil type	1
n° Control volumes	250
Time step simulation	hourly
Initial condition	Hydrostatic with $\psi = 0$ m at the bottom
Top boundary condition	Top Coupled
Bottom boundary condition	Free drainage
Canopy height	3.5 m
LAI	2.5 - 4
Root depth	2 m
Root density	Willow "Spike II" experiment
Type of stress applied	Water stress
$G_{Tw}$	RootDensityWeightedSF
$G_{Ew}$	AverageSF
Transpiration splitter	RootWaterWeightedMethod
Evaporation splitter	AverageWaterWeightedMethod

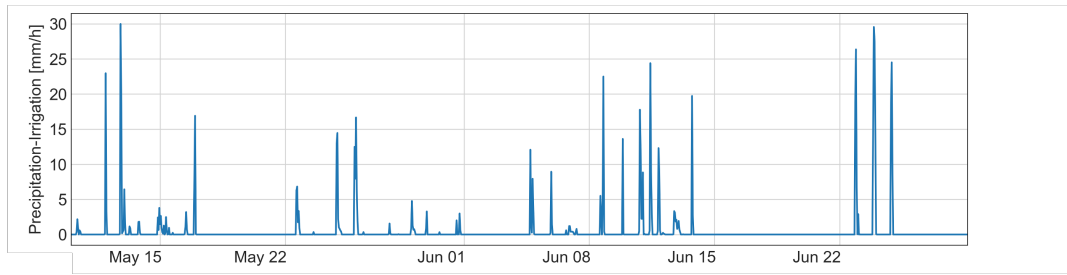
**Table 2.** Hydraulic properties of the soil column for the baseline simulation.

$\theta_r$ [-]	$\theta_s$ [-]	$\theta_{WP}$ [-]	$\theta_{FC}$ [-]	$\alpha$ [ $m^{-1}$ ]	$n$ [-]	$K_s$ [ $m s^{-1}$ ]
0.05	0.3	0.0803	0.205	6	1.31	$3.4722 \times 10^{-5}$

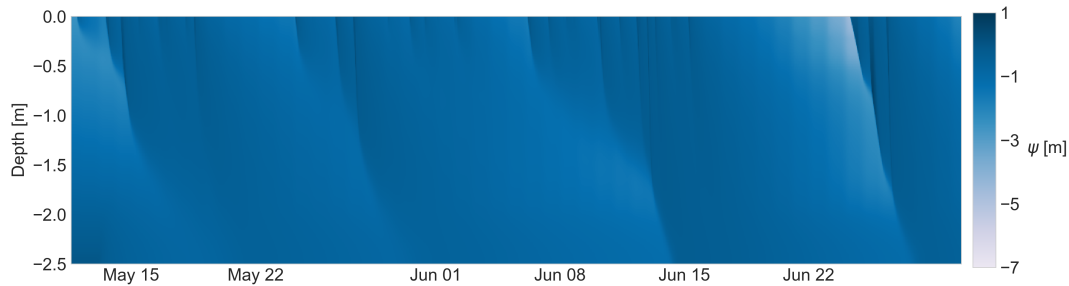
Table 1 provides a comprehensive overview of the settings employed in the baseline simulation. For further details, please refer to the dedicated folder available on the Zenodo repository (D'Amato and Rigon, 2024) and the original Thesis (D'Amato, 2024).

645 Figure 12b depicts the temporal evolution of soil water potential of the BSL simulation following the rainfall event illustrated in Figure 12a . Darker blue patterns indicate higher soil water potential, demonstrating a noticeable increase following irrigation or rainfall episodes. In the last events, saturation occurs, leading to surface ponding, eventually resulting in the formation of an infiltrating saturated front. The above situation is better clarified in Figure 13 where saturation is evident to be generated at the surface (blue line) and quickly propagate in the soil down to -1.5 m.

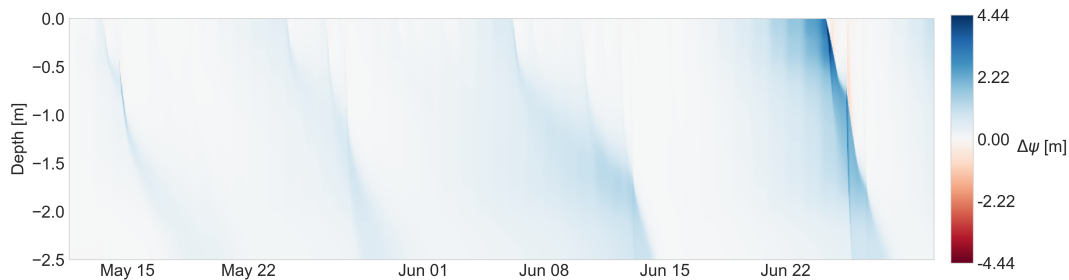
650 **C5-C32** No instabilities along the simulation are visible, even when the systems move from unsaturate to saturate conditions and viceversa, and the mass balance closure is verified being the error in the closure is around  $10^{-9}$  m as shown in the supplemental material.



(a) Precipitation–irrigation input over time.



(b) Soil water potential behavior in the baseline simulation.



(c) Temporal evolution of the soil water potential difference along the soil profile,  $\Delta\psi = \psi_R - \psi_{BSL}$ , where  $\psi_R$  refers to the simulation with infiltration only, and  $\psi_{BSL}$  to the baseline simulation.

**Figure 12. C15** Comparison of soil water potential evolution under scenarios with and without evapotranspiration: Panel (a) shows the precipitation–irrigation input over time. Panel (b) depicts the soil water potential ( $\psi$ ) in the baseline simulation, which includes both infiltration and evapotranspiration. The plot displays depth in meters, with a color scale representing  $\psi$ . C5-C32 The darker blue colors indicate increases in  $\psi$  resulting from rainfall events and their subsequent propagation over time, typically in a downward direction. As depth increases and water potential decreases, infiltration rates slow down due to reduced soil hydraulic conductivity. This phenomenon is visually represented by the decreasing intensity of the darker signatures and their rightward curvature with depth. Panel (c) illustrates the temporal evolution of the soil water potential difference, defined as  $\Delta\psi = \psi_R - \psi_{BSL}$ , where  $\psi_R$  refers to the simulation with infiltration only, and  $\psi_{BSL}$  to the baseline simulation. A diverging colormap centered at zero is used to represent  $\Delta\psi$  values. Positive differences (blue) indicate higher  $\psi_R$  in the infiltration-only case, while negative differences (red) indicate lower  $\psi_R$ . These deviations primarily result from the absence of evapotranspiration in the infiltration-only simulation.

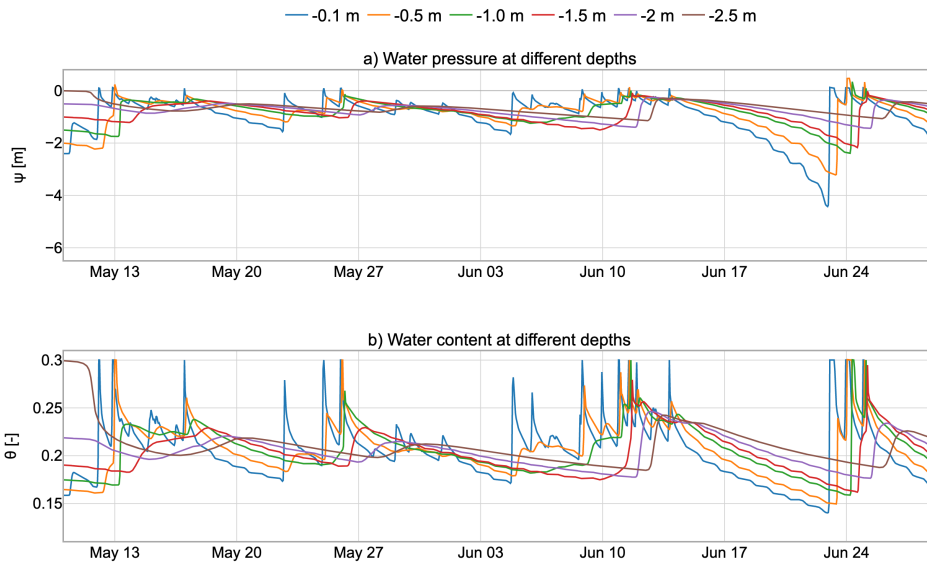


**Figure 13.** (a) Soil water potential, and (b) water content evolution with time at different depth in the baseline simulation. C5-C32 The data in these two figures are clearly related through the soil water retention curve. Notably, following certain rainfall events, soil saturation ( $\psi > 0$ ) is achieved a condition that cannot be adequately handled by solvers less sophisticated than those implemented in GEOSPACE.

As depicted in Figure 14, the GEOSPACE-1D outputs provide the necessary data to visualize water pressure and water content profiles at different time steps. This particular figure represents the scenario estimating the combined effects of infiltration and transpiration on soil moisture.

In the second virtual simulation, we replicated the baseline simulation while excluding the evapotranspiration process, thus following the development of the infiltration process in the soil column without evapotranspiration. The outputs of this simulation are in Figure 15 and Figure 12c. In particular, In contrast, Figure 15 serves as a visual comparison, illustrating the dynamics of infiltration without water extraction by the plant. The increased saturation of the soil column compared to the baseline simulation is particularly evident when comparing Figures 14 and 15. In this scenario, we replicated the baseline simulation while excluding the evapotranspiration process, thus following the development of the infiltration process in the soil column without evapotranspiration. It's evident that the soil column becomes more saturated compared to the baseline simulation. The mass balance closure is usually verified in the simulation and, in this case, the error in the closure is around  $10^{-9}$  m as shown in the supplemental material. The differences between the two cases of infiltration are particularly evident when comparing Figures 14 and 15.

For a more comprehensive analysis, Figure 12c illustrates the temporal evolution of the soil water potential difference along the soil profile, defined as  $\Delta\psi = \psi_R - \psi_{BSL}$ , where  $\psi_R$  refers to the simulation with infiltration only, and  $\psi_{BSL}$  to the baseline simulation with coupled evapotranspiration. This comparison highlights how the exclusion of evapotranspiration processes

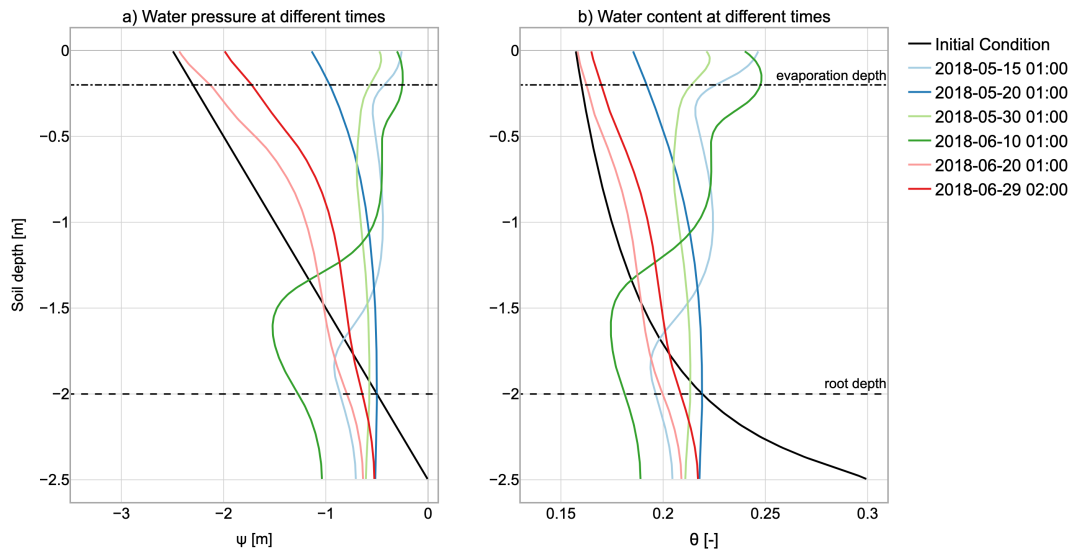


**Figure 14.** (a) Evolution of soil water potential, and (b) water content along the soil profile at various arbitrarily chosen times in the baseline simulation. C5-C32 The initial condition (depicted in black) is hydrostatic but evolves rapidly upon commencement of rainfall. The resulting evolution exhibits a distinct vertical pattern corresponding to the root distribution profile. At the lower portion of the profile, the final conditions are notably influenced by the free drainage boundary condition imposed at the bottom.

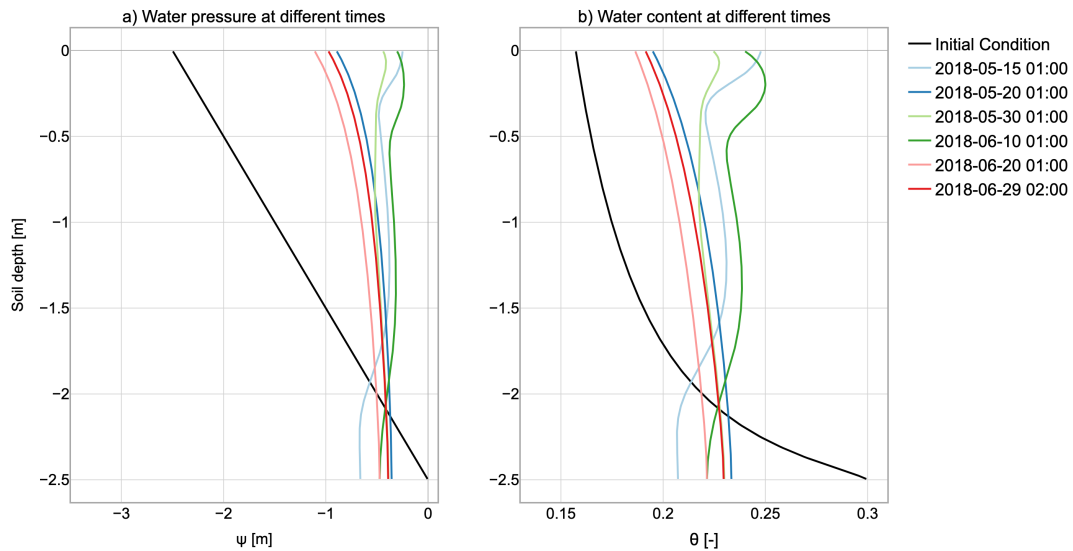


**Figure 15.** (a) Evolution of soil water potential, and (b) water content along the soil profile at various arbitrarily chosen times in a scenario without Evapotranspiration. C5-C32 Under identical initial and lower boundary conditions as the previous figure, this second simulation logically maintains a higher soil water content throughout the profile.

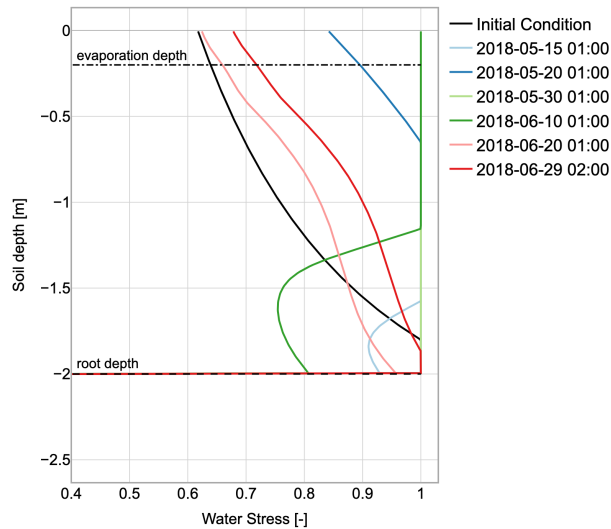


**Figure 16.** Evolution of water stress factor along the soil profile at various arbitrarily chosen times in the baseline simulation. C5-C32 This information can support more accurate and efficient irrigation scheduling based on soil water availability.

670 significantly alters soil water dynamics. In particular, the absence of evapotranspiration results in higher soil water potentials over time, especially in the upper layers, where root water uptake and evaporation typically occur more intensively. These differences amplify with increasing time elapsed since the last precipitation event, creating a cumulative divergence in the soil moisture profile. This divergence becomes less pronounced following new precipitation inputs, which temporarily reduce the evapotranspiration-induced differences by replenishing soil moisture across all simulation scenarios.

it is recommended to compare Figure 12b and 12b.

675 C5-C32 Although a comprehensive analysis of real-world cases exceeds the scope of this paper, our results clearly challenge the conventional "business as usual" simulation approach that estimates infiltration without adequately accounting for plant water uptake. The total bottom flux without evapotranspiration amounts to 602.31 mm, a stark contrast to the 180.09 mm observed in the baseline simulation, resulting in a 234.6% increase in groundwater recharge.

680 Figure 16 represents the evolution of the water stress in time and depth in the BSL. As said before, the root depth is considered constant in time but a time series describing the root depth growth could be provided as an input to the model, if available. The bulk stress factor can be easily estimated from the data provided and is shown in the Zenodo folder material (D'Amato and Rigon, 2024). C5-C32 Unlike conventional modeling practices where irrigation is triggered based on soil water content or soil water potential measurements, GEOSPACE enables direct assessment of water stress levels at any soil depth. However, it is important to note that the current version of the software does not yet incorporate the phenomenon of hydraulic 685 redistribution, whereby roots can redistribute water vertically through the soil profile.

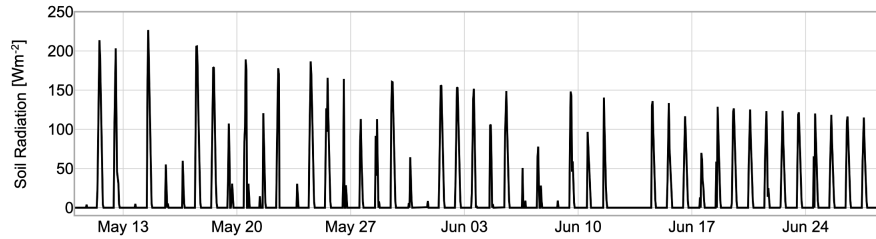


**Figure 17.** Radiation reaching the ground, given the prescribed LAI as input, in the baseline simulation. **C5-C32** Decrease of radiation depends on meteorological conditions and the increase of LAI with time.

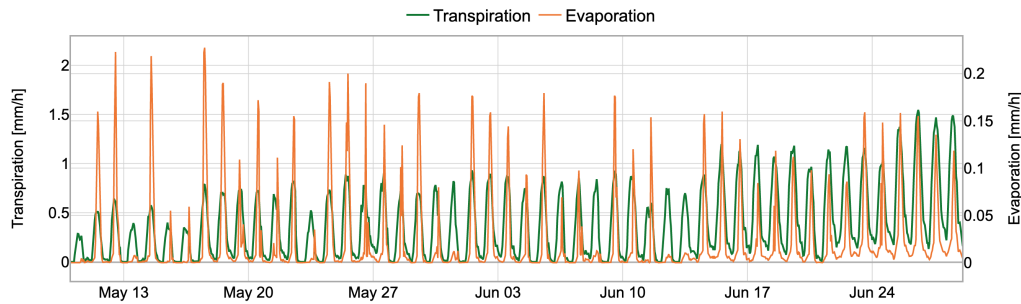


**Figure 18.** Evolution of Transpiration (green) and Evaporation (orange) fluxes with time in the baseline simulation. **C5-C32** The observed increase in transpiration over time results from the concurrent increases in solar radiation approaching the summer solstice, vegetation leaf area index (LAI), and root system expansion.

Solar radiation is measured in this experiment, but it undergoes filtration as it passes through the plant canopy, as described by the model presented in the supplemental material. The remaining radiation, known as residual radiation, is depicted in Figure 17, and it reaches the soil, where it is utilized to estimate soil evaporation using the PM-FAO model. The estimated soil evaporation and transpiration rates are then shown in Figure 18.

## 690 7.1 User information: Input and Output

The GEOSPACE-1D system exhibits a modular structure, necessitating various inputs contingent upon the specific modules employed. Table 3 summarizes the general inputs required for all components in GEOSPACE-1D. These simulation parameters, including the simulation's temporal parameters, are user-defined in the OMS3 .sim file.

695 In the context of WHETGEO, input data can be categorized into two main key components: time series and computational grid data (Table 4). Time series data primarily serve to define the boundary conditions for the case study. These time series are encapsulated within .csv files specific for OMS3 format. Computational grid data encompasses domain discretization, initial conditions, and terrain parameters, all stored in Network Common Data Form (netCDF) files. The processing of time series and computational grid data is executed using specialized Python modules integrated into the `geoframepy` package (Tubini and Rigon, 2021).

700 Specifically, the time series data for boundary conditions needs meteorological information about precipitation, the presence of surface ponding, and the hydraulic condition at the base of the soil column. When addressing computational grid considerations, it is essential to specify the structure of the soil column, such as the soil horizons and hydrological/hydraulic parameters, or to employ literature data for saturated hydraulic conductivity, water content at saturation, residual values, and the water retention curve parameters (SWRC), as outlined in WHETGEO (Tubini, 2021). Most of these soil parameter, implemented as  
705 default in WHETGEO, are available in Bonan (2019), but any other dataset can be used as well by changing the appropriate configuration files.

The input data required by GEOET are time series of meteorological forcings, that could be downloaded from online weather service portals. Specifically, the input data includes time series of air temperature, wind speed, relative humidity, solar radiation, and pressure, but they depend on the evapotranspiration model used from those available (Table 5). In the context of vegetation  
710 characterization, Leaf Area Index data and canopy height, acquired from literature or satellite sources, are fundamental for the computation of transpiration flux. Root depth ( $z_R$ ) and density ( $\delta_R$ ) have to be specified in the creation of computational grid data, because their information is needed in each control volume. Additionally, parameters associated with stress factor calculations, such as the water content at wilting point ( $\theta_{WP}$ ) and field capacity ( $\theta_{FC}$ ), can be readily sourced from available literature. Finally, the user has to specify which model to use to compute the representative water stress factor  $G_w$  (Section 5)  
715 and accordingly, also the model to split evapotranspiration with BrokerGEO (Table 6) as described in Section 6.2. The output data of GEOSPACE-1D depends on the model combination that we use. Table 7 summarizes the GEOSPACE-1D outputs.

The WHETGEO model generates output data in NetCDF format. Nevertheless, these outputs (as well as the inputs) are managed separately by specifically designed OMS3 components, which handle the writing and reading processes. This separation ensures modularity and flexibility, allowing alternative writers and readers to be provided to adapt to different file formats as  
720 required.

For ease of reading, we provide users with extensively commented Python Notebooks, through which all possible outputs of WHETGEO-1D can be accessed. Outputs include water suction [m], water content [-], Darcy velocity [m/s], mass balance error, and others. If the heat transport model is used, the soil temperature is also outputted.

**Table 3.** General inputs required for all components in GEOSPACE-1D. These simulation parameters, including the simulation’s temporal parameters, are user-defined in the OMS3 .sim file.

Temporal Resolution (Minute/Hourly/Daily)	Start-End Date	Point Geographical Location (Long-Lat-Elevation)
--	----------------	---

**Table 4.** Input data for WHETGEO component, categorized into two main elements: time series and computational grid data.

WHETGEO	
Time Series	Top BC Bottom BC Precipitation
Computational grid data	Initial condition ( $\psi_0, T_0, z_R, \delta_R$ ) Soil discretization (depth per each layer) Soil parameters ( $\theta_S, \theta_R, \theta_{WP}, \theta_{FC}, K_s$ ) Soil parameters for SWRC

To date, GEOET results have been stored in OMS3 CSV files, and the type of outputs depends on the evapotranspiration model used in GEOSPACE-1D, as highlighted in Table 7. Specifically, if we consider Prospero for transpiration and Penman-Monteith for soil evaporation, the estimated output quantities are: soil evaporation [mm/time], transpiration [mm/time], latent and sensible heat flux [ $Wm^{-2}$ ], leaf temperature [ $^{\circ}C$ ], water vapor deficit [-], and so on. For a complete description, please refer to the Jupyter Notebook 00\_Notebook of GEOSPACE-1D in the GitHub page model.

It’s important to highlight that a common challenge in conducting simulations is the scarcity of data required to perform them. For instance, obtaining data on root density can be difficult, and it’s not always guaranteed that a study site will have a meteo station providing all the necessary data outlined in Tables 4 and 5. This is why GEOET offers both simple and complex evapotranspiration models. In cases where all the required data for complex models isn’t available, simpler models requiring fewer inputs can be utilized.

Taking again Prospero as an example, it’s possible to encounter situations where only a few of the necessary inputs are missing. In such instances, default data from the model or data from existing literature can be used. In the context of evapotranspiration models, radiation is a critical input that must never be absent, as it serves as the primary driver. Similarly, when it comes to roots, while the depth of roots may be known, their density is often unknown. In such cases, one may opt for an arbitrary distribution or reconstruct it using data from literature or more users can use one of the root density growth methods implemented in GEOET. For more information please refer to D’Amato (2024).

**Table 5.** Time series input data for GEOET component. Comparison of input requirements for different evapotranspiration models (Prospero, PM-FAO, and PT) in GEOET

GEOET			
Input	Prospero	PM-FAO	PT
Air Temperature [°C]	✓	✓	✓
Wind Velocity [m/s]	✓	✓	-
Relative Humidity [-]	✓	✓	-
Net Radiation [ $\text{Wm}^{-2}$ ]	✓	✓	✓
Short Wave Direct [ $\text{Wm}^{-2}$ ]	✓	-	-
Short Wave Diffuse [ $\text{Wm}^{-2}$ ]	✓	-	-
Soil Heat Flux [ $\text{Wm}^{-2}$ ]	✓	✓	✓
Atmospheric Pressure [Pa]	✓	✓	✓
Leaf Area Index [-]	✓	-	-
Canopy height [m]	✓	✓	-
Model to compute $G_{Tw}$ (Section 5)	✓	✓	✓

**Table 6.** Overview of key inputs within the BrokerGEO Model: the algorithm for computing reference evapotranspiration ( $ET_{ref,i}$ ), details about the computational grid, and the reference flux, evaporation, transpiration or evapotranspiration, to be splitted.

BrokerGEO
Model to compute $ET_{ref,i}$ (Section 6.2)
Computational grid information
Reference flux to be splitted (ET)

**Table 7.** GEOSPACE-1D model Outputs: Hydrological and meteorological variables between WHETGEO Output (.netcdf) and GEOET Output (.csv).

<b>WHETGEO Output (.nc)</b>	*Water Suction [m]
	*Water content [-]
	*Darcy velocity [m/s]
	Volume error [m]
	Surface runoff [m/s]
	*Evapotranspiration [m]
	*Water stress [-]

<b>GEOET Output (.csv)</b>	<b>**Prospero + PM</b>	<b>PM-FAO</b>	<b>PT</b>
Latent Heat Sun [ $\text{Wm}^{-2}$ ]	✓	-	-
Latent Heat Shadow [ $\text{Wm}^{-2}$ ]	✓	-	-
Transpiration [mm/time]	✓	-	-
EvapoTranspiration [mm/time]	**✓	✓	✓
Soil Evaporation [mm/time]	**✓	-	-
Leaf Temperature Sun [K]	✓	-	-
Leaf Temperature Shadow [K]	✓	-	-
Sensible Heat Sunlit [ $\text{Wm}^{-2}$ ]	✓	-	-
Sensible Heat Shadow [ $\text{Wm}^{-2}$ ]	✓	-	-
Radiation Soil [ $\text{Wm}^{-2}$ ]	✓	-	-
Radiation Sun [ $\text{Wm}^{-2}$ ]	✓	-	-
Radiation Shadow [ $\text{Wm}^{-2}$ ]	✓	-	-
Canopy [-]	✓	-	-
VPD [-]	✓	-	-

---

\* This variable contains all the output of the current time step  
and for each control volumes.

---

\*\* When we use Prospero, we compute evaporation with PM model  
defining as input an evaporation depth for the soil.

---

## 740 8 User information: Code availability

The latest executable code of only WHETGEO model with the new classes mentioned before can be downloaded from <https://github.com/geoframecomponents/WHETGEO-1D> and can be compiled by following the instructions therein. The version of the OMS3 compiled project can be found at [https://github.com/GEOframeOMSProjects/OMS\\_Project\\_WHETGEO1D](https://github.com/GEOframeOMSProjects/OMS_Project_WHETGEO1D).

745 The Object Modeling System v.3 (OMS3) is a component-based environmental modeling framework introduced by David et al. (2013). More information in the Supplement.

While the majority of the content presented thus far holds broad relevance, it's important to note that the deployment example showcased here pertains to a one-dimensional (1D) context. Comprehensive information on GEOSPACE-1D, intended for both users and developers, can be found in the supplementary materials. Included within is a Jupyter Notebook labeled with the prefix "00\_", affectionately referred to as "Notebook Zero," which serves as a comprehensive guide for executing the code per-  
750 taining to any of the components. The latest executable code can be downloaded from <https://github.com/geoframecomponents/GEOSPACE-1D> and can be compiled by following the instructions therein. Finally, the version of the OMS3 compiled project can be found at [https://github.com/GEOframeOMSProjects/OMS\\_Project\\_GEOSPACE-1D](https://github.com/GEOframeOMSProjects/OMS_Project_GEOSPACE-1D).

The code can be executed in the OMS3 console, which can be downloaded and installed according to the instructions given at <https://geoframe.blogspot.com/2020/01/the-winter-school-on-geoframe-system-is.html>.

755 The various components of GEOSPACE v.1.2.9 are finally compiled and grouped in the following `.jar` files:

- `whetgeo1d-1.2.9` includes the WHETGEO model components;
- `brokergeo-1.3.9` includes the BrokerGEO coupler;
- `geoet-1.5.9` includes the GEOET model containing the ET modules, besides the root functioning, the modules that split the radiation into the canopy and soil layers, the stress factor estimators;
- 760 – `buffer-1.1.9` contains ancillary modules for the management of data in memory and their eventual printing;
- `closureequation-1.1.9` manage the equations that are actually solved in WHETGEO;
- `netcdf-1.1.9` manage the input and output from and to netcdf files;
- `numerical-1.0.2` contains the core algorithms for the solutions of the equations.

The integration of all components took place within the Object Modeling System v3 framework (OMS3) and interlinked  
765 within GEOSPACE. Notably, within the aforementioned components, specific to WHETGEO, are modules such as *buffer*, *closureequation*, *netcdf* and *numerical*. For comprehensive information on these WHETGEO specific components, you can refer to Tubini (2021). Due to the modularity of the system, whilst the components were developed and can be enhanced independently, they can be seamlessly used at run time by connecting them with the OMS3 DSL language based on Groovy. OMS3 provides the basic services and, among them, tools for calibration and implicit parallelization of component runs.

770 Finally more comprehensive information about GEOframe is available at:

– <https://abouthydrology.blogspot.com/2015/03/jgrass-newage-essentials.html>

– <https://geoframe.blogspot.com/2020/01/gsw2020-photos-and-material.html>

## 9 Conclusions

This paper presents and discusses the implementation of the GEOSPACE framework, in particular its one-dimensional development, which stands out among various software for its component-based organization leveraging the OMS3 framework. GEOSPACE-1D comprises three main components: WHETGEO, GEOET, and BrokerGEO. WHETGEO serves as a solver for the Richards-Richardson equation, employing a novel integration algorithm, incorporating the soil energy budget, and featuring automatic switching between saturated and unsaturated conditions. GEOET implements various evapotranspiration formulas and the Prospero model, which concurrently solves transpiration and heat transport alongside the stationary energy budget. Additionally, GEOET provides information on the temperature and water pressure differentials between leaves and air. BrokerGEO acts as a connector between the GEOET and WHETGEO solvers, redistributing evaporation and transpiration demands within the soil column. Additionally, the paper delves into the underlying philosophy of the GEOSPACE framework, which can be succinctly summarized as a structure designed to facilitate modifications aimed at exploring soil-plant-atmosphere interactions under various hypotheses and incorporating new research findings. This objective is accomplished by implementing core functionalities as relationships among abstract objects, specifically interfaces, which are subsequently instantiated into concrete classes, allowing flexibility for user/programmer choices. The instantiation mechanism for these classes is achieved using the factory pattern. A consequence of the above choices is that, for instance, the creation of a new method for estimating the water stress consists in just adding a new class that extends the general interface. Adding a new method for estimating transpiration or evaporation can require a few classes, depending on the complexity of the method, but always obeying the prescription that the code remain “open to extensions and close to modifications”. In the cases already deployed, the Priestley Taylor formulas is implemented by using three classes, while the Prospero model requires a few more as shown in Figure 6. Departing from the strict object-oriented paradigm, which necessitates the creation and destruction of immutable classes, GEOSPACE-1D adopts a more conventional approach, particularly familiar to scientists, for classes dedicated to data containment. Data classes are structured as singletons, instantiated once and continuously updated with new content at each time step.

The model’s capabilities are showcased through a "baseline" simulation, which compares infiltration estimates with and without evaporation and transpiration based on data collected in the "Spike II" experiment at the Ecole Polytechnique Fédérale de Lausanne. The simulations conducted aimed to highlight the functionalities and capabilities of the system, demonstrating its ability to maintain water mass and energy conservation. It’s worth noting that during these simulations, the soil column experiences saturation due to a perched water table while transpiration occurs. Throughout the simulations, the mass budget closure is rigorously monitored and consistently achieved with high precision, despite the diverse range of simulated conditions. These simulations exhibit a strong correspondence with measured data, as further elaborated in a companion paper currently in preparation.

As part of the project, a collection of companion Jupyter Notebooks has been developed to elucidate the process of inputting data required by GEOSPACE-1D, across various configurations. This aligns with the model's implementation philosophy, which separates the handling of model-agnostic components (written in Python and potentially compatible with other modeling platforms) from the model-specific elements (programmed in Java, in our case). The outcome of any simulation setup is encapsulated in OMS3 ".sim" files, facilitating easy sharing. In line with promoting FAIR principles in modeling, all aspects related to GEOSPACE-1D including executables, Notebooks, simulations, input and output data files are consolidated within OMS3 projects and can be readily distributed. Everything utilized in this paper is included in the dedicated folder available on the Zenodo repository (D'Amato and Rigon, 2024) for third-party inspection and self-instruction. Furthermore, the source code is openly accessible and provided on GitHub, as detailed in the relevant sections of the paper. Additionally, instructional videos demonstrating the system's functionality can be found on the GEOframe blog.

*Code availability.* ~~The software is available on the GEOframe Components GitHub repository, as detailed in Section 8.~~ The source code of GEOSPACE, written in Java using an object-oriented programming approach, is specifically hosted on GitHub at <https://github.com/geoframecomponents/GEOSPACE-1D>. Additionally, the corresponding OMS3 project is accessible at [https://github.com/GEOframeOMSProjects/OMS\\_Project\\_GEOSPACE-1D](https://github.com/GEOframeOMSProjects/OMS_Project_GEOSPACE-1D) here. Details about external dependencies are provided in the README file of the GEOSPACE-1D GitHub page.

To execute the code, you must use the OMS3 Console. Instructions for setting up the environment can be found in the README file within the repository. After installing OMS3, follow the guidelines in the Documentation folder, which contains all necessary details about simulation inputs and parameters.

*Data availability.* Data used in this paper is available as part of the "Spike II" tracer experiment dataset (Nehemy et al., 2020), under Creative Commons Attribution (CC BY) license, at <https://doi.org/10.5281/zenodo.4037240>. The simulation presented in this work are available on the Zenodo repository at <https://doi.org/10.5281/zenodo.14269721>.

*Video supplement.* Video illustrating the use of the GEOSPACE-1D parts are present in the material of the GEOframe 2022 Summer School

## 825 **Appendix A: GEOET**

The evapotranspiration component, GEOET, is a deep refactoring of the GEOframe-ETP model (Bottazzi, 2020; Bottazzi et al., 2021). The GEOET framework incorporates four evapotranspiration models, as illustrated in Figure 6. Starting with the simplest model, we have the Priestley-Taylor model (PT), the Penman-Monteith FAO (PM) approximation, an adaptation of the Penman-Monteith model, the Prospero model (Bottazzi, 2020; Bottazzi et al., 2021) and the TranspirationBudget model, a complex computation of the energy budget at the canopy scale described in D'Amato and Rigon (2025). The Priestley-

Taylor model was already fully described in the main text, while the PM model and the Prospero model requires some further explanations.

## A1 Penman-Monteith FAO additional information

Chapter 2 of FAO evapotranspiration book (Food and Agriculture Organization of the United Nations) introduces the user to the need to standardize one method to compute reference evapotranspiration ( $ET_0$ ). As described in Bottazzi (2020), the Penman-Monteith FAO is the approximation for the Penman-Monteith, defined for a reference crop as a hypothetical crop with an assumed height of 0.12 m, having a surface resistance of  $70 \text{ s m}^{-1}$  and an albedo of 0.23. It is widely used especially in agricultural field.

Starting from the Penman-Monteith equation, the FAO approximation for a grass reference surface lead to computation of a reference evapotranspiration as follow:

$$ET_0 = \frac{1}{\lambda} \frac{0.408\Delta(R_n - G) + \gamma \frac{900}{T+273} u_2 (e_s - e_a)}{\Delta + \gamma(1 + 0.34u_2)} \quad (\text{A1})$$

where:  $ET_0$  is the reference evapotranspiration [ $\text{mm day}^{-1}$ ],  $R_n$  is the net radiation at the crop surface [ $\text{MJ m}^{-2} \text{ day}^{-1}$ ],  $G$  is the soil heat flux density [ $\text{MJ m}^{-2} \text{ day}^{-1}$ ],  $T$  is the mean daily air temperature at 2 m height [ $^{\circ}\text{C}$ ],  $u_2$  is the wind speed at 2 m height [ $\text{m s}^{-1}$ ],  $e_s$  is the saturation vapour pressure [ $\text{kPa}$ ],  $e_a$  is the actual vapour pressure [ $\text{kPa}$ ],  $(e_s - e_a)$  is the saturation vapour pressure deficit [ $\text{kPa}$ ], and  $D$  is the slope vapour pressure curve [ $\text{kPa } ^{\circ}\text{C}^{-1}$ ],

Using the latent heat constant  $\lambda$ , the reference evapotranspiration can be converted to the reference latent heat:

$$E_0 = ET_0 \cdot \lambda \quad (\text{A2})$$

FAO computes the actual evapotranspiration using the water stress coefficient  $K_s$  and the single crop coefficient  $K_c$ :

$$E_{FAO} = ET_0 \cdot K_s \cdot K_c \quad (\text{A3})$$

Values for  $K_c$  are given by FAO in Table 12 of Chapter 6. The water stress coefficient  $K_s$  can be computed as:

$$K_s = \frac{TAW - D_r}{TAW - RAW} = \frac{TAW - D_r}{(1 - p)TAW} \quad (\text{A4})$$

$$RAW = p \cdot TAW \quad (\text{A5})$$

$$TAW = 1000(\theta_{FC} - \theta_{WP}) \cdot Z_r \quad (\text{A6})$$

$$TAW = 1000(\theta_{FC} - \theta) \cdot Z_r \quad (A7)$$

855 where:

- $K_s$  is a dimensionless transpiration reduction factor dependent on available soil water [0 - 1];
- $D_r$  root zone depletion [mm];
- $TAW$  total available soil water in the root zone [mm];
- $p$  fraction of  $TAW$  that a crop can extract from the root zone without suffering water stress [-];
- 860 –  $\theta_{FC}$  the water content at field capacity [ $\text{m}^3\text{m}^{-3}$ ];
- $\theta_{WP}$  the water content at wilting point [ $\text{m}^3\text{m}^{-3}$ ];
- $\theta_{WP}$  the measured water content [ $\text{m}^3\text{m}^{-3}$ ];
- $Z_r$  the rooting depth [m].

## A2 Prospero model

865 The Prospero model, Bottazzi (2020) and Bottazzi et al. (2021), is a physically based approach for calculating canopies transpiration ( $T$ ) and soil evaporation  $E$ . These processes are considered for both sunlit and shaded fractions of the canopy.  $E$  from the soil is determined according the FAO Penman–Monteith model meanwhile,  $T$  is computed using a modified version of the Schymanski and Or (Schymanski and Or, 2017) (SO) model, which has been upscaled to address canopy-level transpiration and modified to ensure mass conservation during periods of water stress. SO model solves the stationary energy budget coupled with the water vapor transport Dalton’s equation and the sensible heat  $S$  equation by using a suitable simplification of the  
870 Clausius-Clapeyron formula.

For a more in-depth exploration of this topic, readers are encouraged to refer to the comprehensive information provided in Bottazzi (2020) or to D’Amato and Rigon (2025).

To expand the applicability of this equation to the canopy, Bottazzi (2020) chose to implement a two-big-leaf approach (Dai  
875 et al., 2004; Luo et al., 2018), utilizing the Sun/Shade model introduced by (de Pury and Farquhar, 1997) and illustrated in the Supplement. This approach enables the calculation of the fraction of the canopy exposed to direct sunlit and the fraction in shade, along with the radiation absorbed by various canopy layers. Specifically, Prospero employs this two-leaf sun-shade approach, while treating the soil as an additional layer. Other environmental variables such as air temperature, relative humidity, wind, and longwave radiation are assumed to remain constant within the canopy, allowing it to be treated as a single large leaf  
880 emitting latent heat proportionate to its area and shortwave radiation.

The SO approach overcomes several limitations of the Penman-Monteith equation, particularly in its representation of transpiring leaf area and leaf thermal capacity, along with their feedback on the energy balance. Incorrectly representing the transpiring leaf area can significantly impact the overall energy balance. Consequently, the energy budget can be reformulated in terms of the area capable of exchanging fluxes and the equilibrium leaf temperature as follows:

$$885 \quad R_s = a_{sH} A_{tr} R_{ll}(T_l) + a_{sE} A_{tr} E_l(T_l) + a_{sH} A_{tr} H_l(T_l) \quad (A8)$$

where

- $a_{sH}$  is the side of the surface exchanging sensible heat (1 for soil, 2 for leaves) [-],
- $a_{sE}$  is the side of the surface exchanging latent heat (1 for amphistomatous leaves) [-],
- $A_{tr}$  is the area exchanging fluxes (radiation, sensible and latent heat) [ $\text{m}^2\text{m}^{-2}$ ],
- 890 –  $T_l$  is the equilibrium leaf temperature [K].

where the longwave in computed as

$$R_{ll} = a_{sH} A_{tr} \epsilon_l \sigma (T_l^4 - T_a^4) \quad (A9)$$

and T is computed as

$$E_l = c_E(a_{sE}, A_{tr}) \cdot [\Delta(T_l - T_a) + P_{ws} - P_w] \quad (A10)$$

895 the sensible heat is computed as

$$H_l = c_H(a_{sH}, A_{tr}) \cdot [(T_l - T_a)] \quad (A11)$$

$A_{tr}$  is the transpiring surface for unit of ground surface [-],  $a_{sE}$  are the sides of surface exchanging latent heat, equal to 1 for hypostomatous, 2 for amphistomatous [-];  $a_{sH}$  are the sides of surface exchanging sensible heat and longwave radiation, equal to 1 for soil, 2 for leaves [-];  $P_{ws}$  and  $P_w$  are the saturation water vapour pressure and the water vapour pressure. Eventually,

900 the leaf temperature (for each layer treated)  $T_l$  is computed as,

$$T_l = \frac{R_s + a_{sH} A_{tr} \epsilon_l \sigma T_a^4 + c_H(a_{sH}, A_{tr}) \cdot T_a + c_E(a_{sE}, A_{tr}, g_s) \cdot (\Delta e \cdot T_a + P_w - P_{ws})}{c_H(a_{sH}, A_{tr}) + c_E(a_{sE}, A_{tr}, g_s) \Delta e + a_{sH} A_{tr} \epsilon_l \sigma T^3} \quad (A12)$$

where  $g_s$  is the stomatal conductance [ $\text{m s}^{-1}$ ].

### A3 GEOET Classes in detail

The refactoring of the GEOET codes cover some substantial software engineering aspects that are detailed below for some of

905 the packages.

## Working details of the classe `geoet . data` and `geoet . inout`

Parameters, ProblemQuantities, InputTimeSeries are the pivotal data classes that are used by algorithmic classes to get the simulation done. Their relations to form a working program are illustrated in the UML diagrams presented in Figures 5, A1, A2. An identical pattern emerges in the relationships between the method ET solvers and the classes encapsu-  
910 lated within the `geoet . data` and `geoet . inout` packages. To illustrate this point, we will examine the connection between a solver class, such as *PriestleyTaylorActualSolverMain* and the *Parameters* class (Figure 5). The relationship between these classes can be considered both an *association* and an *aggregation*. It is an association because *PriestleyTaylorActualSolverMain* object uses the *Parameters* object only temporarily and is not responsible for its creation or lifecycle management. In fact, *PriestleyTaylorActualSolverMain* has a reference to *Parameters* to access its data, and *Parameters* exists independently  
915 of *PriestleyTaylorActualSolverMain*. But the relation is also an aggregation due to the class *PriestleyTaylorActualSolverMain* contains a field *parameters* of type *Parameters*, and this relationship indicates that *PriestleyTaylorActualSolverMain* "contains" an object of type *Parameters*. The important point is that the *Parameters* class is used by *PriestleyTaylorActualSolverMain* but exists independently of it.

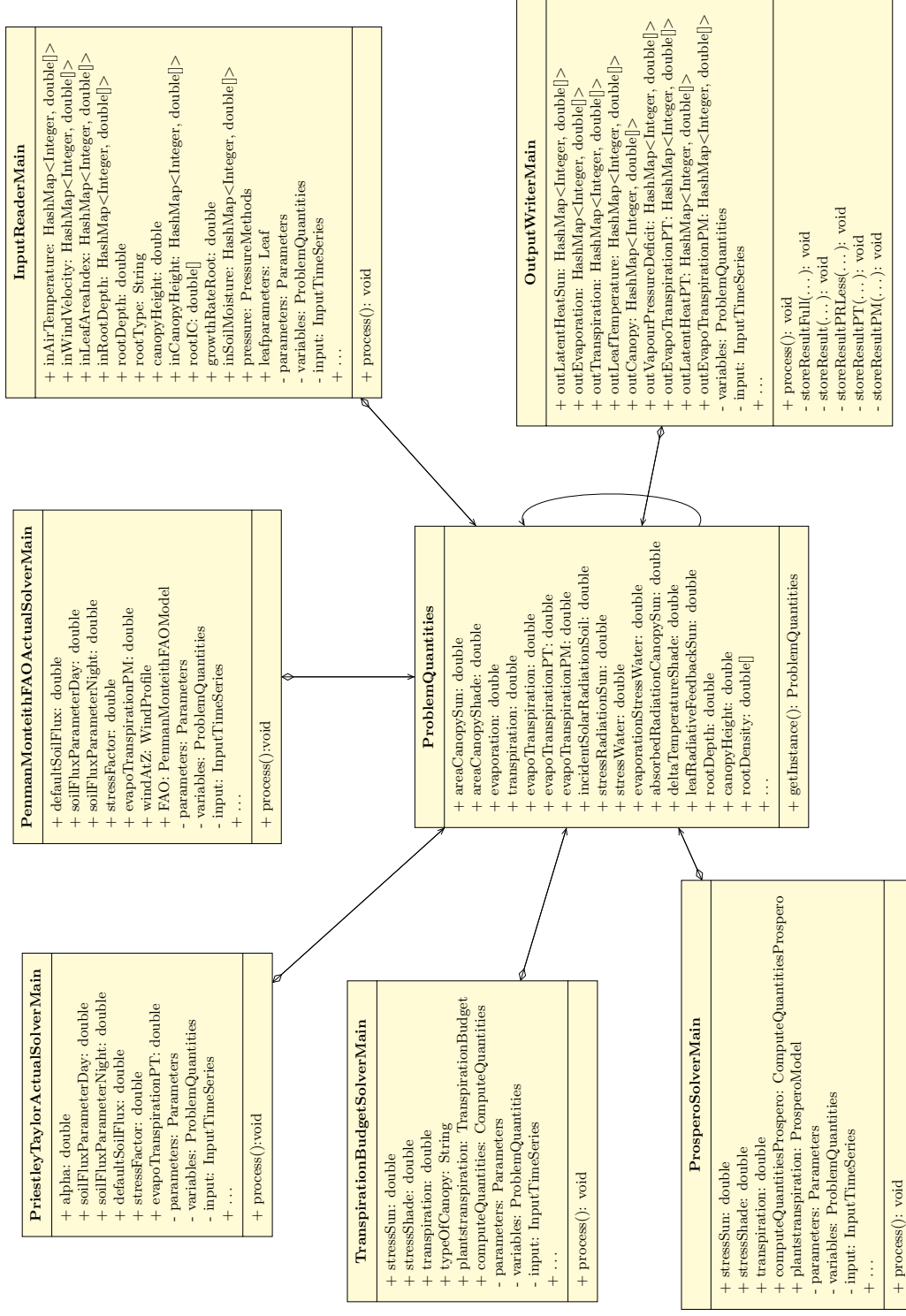


**Figure A1.** UML class diagram for the `ProblemQuantities` class, illustrating the aggregation and association relations with the ET models solvers classes and mainly with the input and output classes. In this way we ensure that all model variables are shared among all classes regardless of the type of ET model used.

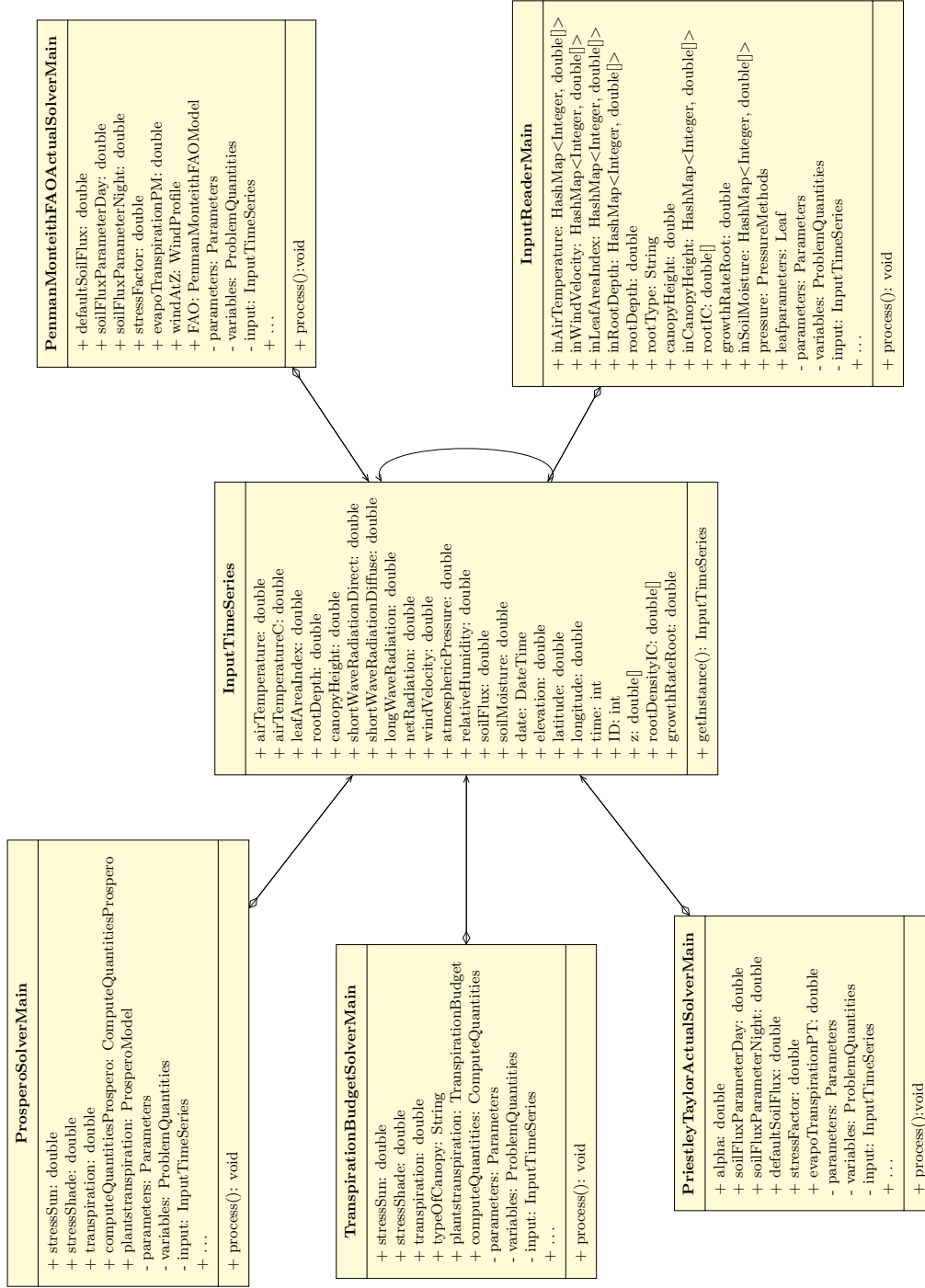


**Figure A2.** UML class diagram for the InputTimeSeries class, revealing the aggregation and association relations with some of the classes involved.

*Author contributions.* CD, RR and NT conceptualized the model’s structure. NT implemented WHETGEO and several foundational classes  
920 crucial for the development of GEOSPACE-1D. Additionally, CD led the refactoring of ETP-GEOFRAME into GEOET, designed and  
implemented BrokerGEO and run the simulations. RR supervised the work of NT and CD and provided financial support. CD and RR  
collaborated on writing the paper and discussed any of its part.

*Competing interests.* There are no competing interest

*Disclaimer.* The software is provided under GPL 3.0 without any responsibility about its use.

925 *Acknowledgements.* This work has been supported by a Ph.D. grant by the Center Agriculture Food Environment - C3A at the University  
of Trento, by the Italian MIUR Project (PRIN 2017) “WATER mixing in the critical ZONE: observations and predictions under environmental  
changes-WATZON” (project code: 2017SL7ABC), by MIUR Project (PRIN 2020) “Unravelling interactions between WATER and carbon  
cycles during drought and their impact on water resources and forest and grassland ecosySTEMs in the Mediterranean climate (WATER-  
STEM) ” (protocol code: 20202WF53Z), and by COST Action WATSON (WATER isotopeS in the critical zONe from groundwater recharge  
930 to plant transpiration), CA19120 supported by COST (European Cooperation in Science and Technology), [www.cost.eu](http://www.cost.eu).

## References

- Allen, R. G., Pereira, L. S., Raes, D., and Smith, M.: Crop evapotranspiration—Guidelines for computing crop water requirements—FAO Irrigation and drainage paper 56, vol. 56, FAO Rome, 1998.
- Anderson, M. C., Kustas, W. P., and Norman, J. M.: Upscaling and downscaling—A regional view of the soil–plant–atmosphere continuum, *Agron. J.*, 95, 1408–1423, 2003.
- Argent, R. M.: An overview of model integration for environmental applications—components, frameworks and semantics, *Environmental Modelling & Software*, 19, 219–234, 2004.
- Asadollahi, M., Nehemy, M. F., McDonnell, J. J., Rinaldo, A., and Benettin, P.: Toward a closure of catchment mass balance: Insight on the missing link from a vegetated lysimeter, *Water Resour. Res.*, 58, 2022.
- 940 Ball, J. T., Woodrow, I. E., and Berry, J. A.: A Model Predicting Stomatal Conductance and its Contribution to the Control of Photosynthesis under Different Environmental Conditions, in: *Progress in Photosynthesis Research: Volume 4 Proceedings of the VIIth International Congress on Photosynthesis Providence, Rhode Island, USA, August 10–15, 1986*, edited by Biggins, J., pp. 221–224, Springer Netherlands, Dordrecht, 1987.
- Bancheri, M., Rigon, R., and Manfreda, S.: The GEOframe-NewAge Modelling System Applied in a Data Scarce Environment, *Water*, 12, 945 86, 2020.
- Benettin, P., Queloz, P., Bensimon, M., McDonnell, J. J., and Rinaldo, A.: Velocities, residence times, tracer breakthroughs in a vegetated lysimeter: a multitracer experiment, *Water Resources Research*, 55, 21–33, <https://doi.org/10.1029/2018wr023894>, 2019.
- Benettin, P., Nehemy, M. F., Asadollahi, M., Pratt, D., Bensimon, M., McDonnell, J. J., and Rinaldo, A.: Tracing and closing the water balance in a vegetated lysimeter, *Water Resour. Res.*, 57, 2021a.
- 950 Benettin, P., Nehemy, M. F., Cernusak, L. A., Kahmen, A., and McDonnell, J. J.: On the use of leaf water to determine plant water source A proof of concept, *Hydrological Processes*, 35, 2021b.
- Berti, G.: Generic software components for Scientific Computing, Ph.D. thesis, Naturwissenschaften und Informatik der Brandenburgischen Technischen Universität Cottbus, 2000.
- Beyer, M., Hamutoko, J. T., Wanke, H., Gaj, M., and Koeniger, P.: Examination of deep root water uptake using anomalies of soil water 955 stable isotopes, depth-controlled isotopic labeling and mixing models, *J. Hydrol.*, 566, 122–136, 2018.
- Bierkens, M. F. P.: Global hydrology 2015: State, trends, and directions, *Water Resour. Res.*, 51, 4923–4947, 2015.
- Blyth, E. M., Arora, V. K., Clark, D. B., Dadson, S. J., De Kauwe, M. G., Lawrence, D. M., Melton, J. R., Pongratz, J., Turton, R. H., Yoshimura, K., and Yuan, H.: Advances in Land Surface Modelling, *Current Climate Change Reports*, 7, 45–71, 2021.
- Bonan, G.: *Climate Change and Terrestrial Ecosystem Modeling*, Cambridge University Press, 2019.
- 960 Bonan, G. B., Lucier, O., Coen, D. R., Foster, A. C., Shuman, J. K., Laguë, M. M., Swann, A. L. S., Lombardozi, D. L., Wieder, W. R., Dahlin, K. M., Rocha, A. V., and SanClements, M. D.: Reimagining Earth in the Earth system, *J. Adv. Model. Earth Syst.*, 16, 2024.
- Bottazzi, M.: Transpiration theory and the Prospero component of GEOframe, Ph.D. thesis, University of Trento, 2020.
- Bottazzi, M., Bancheri, M., Mobilia, M., Bertoldi, G., Longobardi, A., and Rigon, R.: Comparing evapotranspiration estimates from the GEOframe-Prospero model with Penman–Monteith and Priestley–Taylor approaches under different climate conditions, *Water*, 13, 1221, 965 2021.
- Brunet, Y.: Turbulent Flow in Plant Canopies: Historical Perspective and Overview, *Bound.-Layer Meteorol.*, 177, 315–364, 2020.

- Carminati, A. and Javaux, M.: Soil Rather Than Xylem Vulnerability Controls Stomatal Response to Drought, *Trends Plant Sci.*, 25, 868–880, 2020.
- 970 Cassiani, G., Boaga, J., Vanella, D., Perri, M. T., and Consoli, S.: Monitoring and modelling of soil–plant interactions: the joint use of ERT, sap flow and eddy covariance data to characterize the volume of an orange tree root zone, *Hydrol. Earth Syst. Sci.*, 19, 2213–2225, 2015.
- Casulli, V. and Zanolli, P.: High resolution methods for multidimensional advection–diffusion problems in free-surface hydrodynamics, *Ocean Model.*, 10, 137–151, 2005.
- Casulli, V. and Zanolli, P.: A Nested Newton-Type Algorithm for Finite Volume Methods Solving Richards’ Equation in Mixed Form, *SIAM J. Sci. Comput.*, 32, 2255–2273, 2010.
- 975 Chen, M., Voinov, A., Ames, D. P., Kettner, A. J., Goodall, J. L., Jakeman, A. J., Barton, M. C., Harpham, Q., Cuddy, S. M., DeLuca, C., Yue, S., Wang, J., Zhang, F., Wen, Y., and Lü, G.: Position paper: Open web-distributed integrated geographic modelling and simulation to enable broader participation and applications, *Earth Sci. Rev.*, 207, 103 223, 2020.
- Collins, N., Theurich, G., DeLuca, C., Suarez, M., Trayanov, A., Balaji, V., Li, P., Yang, W., Hill, C., and da Silva, A.: Design and Implementation of Components in the Earth System Modeling Framework, *Int. J. High Perform. Comput. Appl.*, 19, 341–350, 2005.
- 980 Craig, J. R., Brown, G., Chlumsky, R., Jenkinson, R. W., Jost, G., Lee, K., Mai, J., Serrer, M., Sgro, N., Shafii, M., Snowdon, A. P., and Tolson, B. A.: Flexible watershed simulation with the Raven hydrological modelling framework, *Environmental Modelling & Software*, 129, 104 728, 2020.
- Cranko Page, J., Abramowitz, G., De Kauwe, M. G., and Pitman, A. J.: Are Plant Functional Types fit for purpose?, *Geophys. Res. Lett.*, 51, 2024.
- 985 Dai, Y., Dickinson, R. E., and Wang, Y.-P.: A Two-Big-Leaf Model for Canopy Temperature, Photosynthesis, and Stomatal Conductance, *J. Clim.*, 17, 2281–2299, 2004.
- Daly, E., Porporato, A., and Rodriguez-Iturbe, I.: Coupled Dynamics of Photosynthesis, Transpiration, and Soil Water Balance. Part II: Stochastic Analysis and Ecohydrological Significance, *J. Hydrometeorol.*, 5, 559–566, 2004.
- D’Amato, C.: Exploring the Soil-Plant-Atmosphere Continuum: Advancements, Integrated Modeling and Ecohydrological Insights, Ph.D. thesis, Center Agriculture Food Environment (C3A), University of Trento, 2024.
- 990 D’Amato, C. and Rigon, R.: Ecohydrological simulation using GEOSPACE-1D model, <https://doi.org/10.5281/zenodo.14269721>, 2024.
- D’Amato, C. and Rigon, R.: Elementary Mathematics Helps to Shed Light on the Transpiration Budget Under Water Stress, *Ecohydrology*, 18, e70 009, 2025.
- David, O., Ascough, J. C., Lloyd, W., Green, T. R., Rojas, K. W., Leavesley, G. H., and Ahuja, L. R.: A software engineering perspective on environmental modeling framework design: The Object Modeling System, *Environmental Modelling & Software*, 39, 201–213, 2013.
- 995 David, O., Lloyd, W., Rojas, K., Arabi, M., Geter, F., Ascough, J., Green, T., Leavesley, G., and Carlson, J.: Modeling-as-a-Service (MaaS) using the Cloud Services Innovation Platform (CSIP), in: International Congress on Environmental Modelling and Software, [scholar.archive.byu.edu](http://scholar.archive.byu.edu), 2014.
- de Pury, D. G. G.: SCALING PHOTOSYNTHESIS AND WATER USE FROM LEAVES TO PADDOCKS, Ph.D. thesis, The Australian National University, 1995.
- 1000 de Pury, D. G. G. and Farquhar, G. D.: Simple scaling of photosynthesis from leaves to canopies without the errors of big-leaf models, *Plant Cell Environ.*, 20, 537–557, 1997.
- Dewar, R. C.: The Ball-Berry-Leuning and Tardieu-Davies stomatal models: synthesis and extension within a spatially aggregated picture of guard cell function, *Plant Cell Environ.*, 25, 1383–1398, 2002.

- 1005 Donovan, L. A. and Sperry, J.: Scaling the soil–plant–atmosphere continuum: from physics to ecosystems, *Trends Plant Sci.*, 5, 510–512, 2000.
- Evaristo, J. and McDonnell, J. J.: Prevalence and magnitude of groundwater use by vegetation: a global stable isotope meta-analysis, *Sci. Rep.*, 7, 44 110, 2017.
- Fatichi, S., Vivoni, E. R., Ogden, F. L., Ivanov, V. Y., Mirus, B., Gochis, D., Downer, C. W., Camporese, M., Davison, J. H., Ebel, B., et al.:  
1010 An overview of current applications, challenges, and future trends in distributed process-based models in hydrology, *Journal of Hydrology*, 537, 45–60, 2016.
- Feddes, R. A., Kowalik, P., Kolinska-Malinka, K., and Zaradny, H.: Simulation of field water uptake by plants using a soil water dependent root extraction function, *J. Hydrol.*, 31, 13–26, 1976.
- Finnigan, J. J., Shaw, R. H., and Patton, E. G.: Turbulence structure above a vegetation canopy, *J. Fluid Mech.*, 637, 387–424, 2009.
- 1015 Fisher, R. A. and Koven, C. D.: Perspectives on the future of land surface models and the challenges of representing complex terrestrial systems, *J. Adv. Model. Earth Syst.*, 12, 2020.
- Formetta, G., Antonello, A., Franceschi, S., David, O., and Rigon, R.: Hydrological modelling with components: A GIS-based open-source framework, *Environmental Modelling & Software*, 55, 190–200, 2014.
- Fowler, M.: *UML Distilled: A Brief Guide to the Standard Object Modeling Language*, Addison-Wesley Professional, 2004.
- 1020 Freeman, E., Robson, E., Bates, B., and Sierra, K.: *Head first design patterns*, O’Reilly Media, Inc.", 2008.
- G., A. R.: A Penman for All Seasons, *J. Irrig. Drain. Eng.*, 112, 348–368, 1986.
- Gamma, E., Helm, R., Johnson, R., . Johnson, R. E., and Vlissides, J.: *Design Patterns: Elements of Reusable Object-Oriented Software*, Pearson Deutschland GmbH, 1995.
- Gardner, H. and Manduchi, G.: *Design Patterns for e-Science*, Springer Science & Business Media, 2007.
- 1025 Giraud, M., Gall, S. L., Harings, M., Javaux, M., Leitner, D., Meunier, F., Rothfuss, Y., van Dusschoten, D., Vanderborght, J., Vereecken, H., Lobet, G., and Schnepf, A.: CPlantBox: a fully coupled modelling platform for the water and carbon fluxes in the soil–plant–atmosphere continuum, in *silico Plants*, 5, diad009, 2023.
- Holling, C. S.: *Adaptive Environmental Assessment and Management*, International Institute for Applied Systems Analysis, 1978.
- Jarvis, P. G., Monteith, J. L., and Weatherley, P. E.: The interpretation of the variations in leaf water potential and stomatal conductance found  
1030 in canopies in the field, *Philos. Trans. R. Soc. Lond. B Biol. Sci.*, 273, 593–610, 1976.
- Katul, G., Lai, C.-T., Schäfer, K., Vidakovic, B., Albertson, J., Ellsworth, D., and Oren, R.: Multiscale analysis of vegetation surface fluxes: from seconds to years, *Adv. Water Resour.*, 24, 1119–1132, 2001.
- Katul, G. G., Oren, R., Manzoni, S., Higgins, C., and Parlange, M. B.: Evapotranspiration: A Process Driving Mass Transport and Energy Exchange in the Soil-Plant-Atmosphere-Climate System, *Rev. Geophys.*, 50, 2012.
- 1035 Kerches Braghieri, R.: *Improving the treatment of vegetation canopy architecture in radiative transfer schemes*, Ph.D. thesis, University of Reading, 2018.
- Kramer, P. J.: Plant and Soil Water Relationships: A Modern Synthesis, *Q. Rev. Biol.*, 45, 218–218, 1970.
- Lai, C.-T. and Katul, G.: The dynamic role of root-water uptake in coupling potential to actual transpiration, *Adv. Water Resour.*, 23, 427–439, 2000.
- 1040 Lehmann, A., Giuliani, G., Ray, N., Rahman, K., Abbaspour, K. C., Nativi, S., Craglia, M., Cripe, D., Quevauviller, P., and Beniston, M.: Reviewing innovative Earth observation solutions for filling science-policy gaps in hydrology, *J. Hydrol.*, 518, 267–277, 2014.
- Leuning, R.: Modelling Stomatal Behaviour and and Photosynthesis of *Eucalyptus grandis*, *Funct. Plant Biol.*, 17, 159–175, 1990.

- Lhomme, J.-P.: Stomatal control of transpiration: Examination of the Jarvis-type representation of canopy resistance in relation to humidity, *Water Resour. Res.*, 37, 689–699, 2001.
- 1045 Li, L., Yang, Z.-L., Matheny, A. M., Zheng, H., Swenson, S. C., Lawrence, D. M., Barlage, M., Yan, B., McDowell, N. G., and Leung, L. R.: Representation of plant hydraulics in the Noah<sup>+</sup>MP land surface model: Model development and multiscale evaluation, *J. Adv. Model. Earth Syst.*, 13, 2021.
- Lin, Y.-S., Medlyn, B. E., Duursma, R. A., Prentice, I. C., Wang, H., Baig, S., Eamus, D., de Dios, V. R., Mitchell, P., Ellsworth, D. S., de Beeck, M. O., Wallin, G., Uddling, J., Tarvainen, L., Linderson, M.-L., Cernusak, L. A., Nippert, J. B., Ocheltree, T. W., Tissue, D. T.,  
1050 Martin-StPaul, N. K., Rogers, A., Warren, J. M., De Angelis, P., Hikosaka, K., Han, Q., Onoda, Y., Gimeno, T. E., Barton, C. V. M., Bennie, J., Bonal, D., Bosc, A., Löw, M., Macinins-Ng, C., Rey, A., Rowland, L., Setterfield, S. A., Tausz-Posch, S., Zaragoza-Castells, J., Broadmeadow, M. S. J., Drake, J. E., Freeman, M., Ghannoum, O., Hutley, L. B., Kelly, J. W., Kikuzawa, K., Kolari, P., Koyama, K., Limousin, J.-M., Meir, P., Lola da Costa, A. C., Mikkelsen, T. N., Salinas, N., Sun, W., and Wingate, L.: Optimal stomatal behaviour around the world, *Nat. Clim. Chang.*, 5, 459–464, 2015.
- 1055 Lloyd, W., David, O., Ascough, J. C., Rojas, K. W., Carlson, J. R., Leavesley, G. H., Krause, P., Green, T. R., and Ahuja, L. R.: Environmental modeling framework invasiveness: Analysis and implications, *Environmental Modelling & Software*, 26, 1240–1250, 2011.
- Luo, X., Chen, J. M., Liu, J., Black, T. A., Croft, H., Staebler, R., He, L., Arain, M. A., Chen, B., Mo, G., Gonsamo, A., and McCaughey, H.: Comparison of Big-Leaf, Two-Big-Leaf, and Two-Leaf Upscaling Schemes for Evapotranspiration Estimation Using Coupled Carbon-Water Modeling, *American Geophysical Union*, 2018.
- 1060 Macfarlane, C., White, D. A., and Adams, M. A.: The apparent feed-forward response to vapour pressure deficit of stomata in droughted, field-grown *Eucalyptus globulus* Labill, *Plant Cell Environ.*, 27, 1268–1280, 2004.
- Manoli, G., Huang, C.-W., Bonetti, S., Domec, J.-C., Marani, M., and Katul, G.: Competition for light and water in a coupled soil-plant system, *Adv. Water Resour.*, 108, 216–230, 2017.
- Mauder, M., Foken, T., and Cuxart, J.: Surface-Energy-Balance Closure over Land: A Review, *Bound.-Layer Meteorol.*, 177, 395–426, 2020.
- 1065 McDermid, S. S., Mearns, L. O., and Ruane, A. C.: Representing agriculture in Earth System Models: Approaches and priorities for development, *J. Adv. Model. Earth Syst.*, 9, 2230–2265, 2017.
- McGrath, M. J., Ryder, J., Pinty, B., Otto, J., Naudts, K., Valade, A., Chen, Y., Weedon, J., and Luysaert, S.: A multi-level canopy radiative transfer scheme for ORCHIDEE (SVN r2566), based on a domain-averaged structure factor, *Climate and Earth System Modeling*, 2016.
- Medlyn, B. E., Duursma, R. A., Eamus, D., Ellsworth, D. S., Prentice, I. C., Barton, C. V. M., Crous, K. Y., de Angelis, P., Freeman, M., and  
1070 Wingate, L.: Reconciling the optimal and empirical approaches to modelling stomatal conductance, *Glob. Chang. Biol.*, 17, 2134–2144, 2011.
- Mencuccini, M., Manzoni, S., and Christoffersen, B.: Modelling water fluxes in plants: from tissues to biosphere, *New Phytol.*, 222, 1207–1222, 2019.
- Miralles, D. G., Vilà-Guerau de Arellano, J., McVicar, T. R., and Mahecha, M. D.: Vegetation-climate feedbacks across scales, *Ann. N. Y. Acad. Sci.*, 1544, 27–41, 2025.
- 1075 Molz, F. J.: Models of water transport in the soil-plant system: A review, *Water Resour. Res.*, 17, 1245–1260, 1981.
- Molz, F. J. and Remson, I.: Extraction term models of soil moisture use by transpiring plants, *Water Resour. Res.*, 6, 1346–1356, 1970.
- Moore, R. V. and Hughes, A. G.: *Integrated environmental modelling: achieving the vision*, Geological Society, London, Special Publications, 408, 17–34, 2017.

- 1080 National Research Council, Commission on Geosciences, Environment, and Resources, Board on Earth Sciences and Resources, and Committee on Basic Research Opportunities in the Earth Sciences: Basic Research Opportunities in Earth Science, National Academies Press, 2001.
- Nehemy, M. F., Benettin, P., Asadollahi, M., Pratt, D., Rinaldo, A., and McDonnell, J. J.: Dataset: The SPIKE II experiment - Tracing the water balance, <https://doi.org/10.5281/zenodo.4037240>, data set, 2020.
- 1085 Nehemy, M. F., Benettin, P., Asadollahi, M., Pratt, D., Rinaldo, A., and McDonnell, J. J.: Tree water deficit and dynamic source water partitioning, *Hydrol. Process.*, 35, 2021.
- Nilsen, E. and Orcutt, D.: *The Physiology of Plants Under Stress, Abiotic Factors*, Wiley, 1996.
- Overgaard, J., Rosbjerg, D., and Butts, M. B.: Land-surface modelling in hydrological perspective – a review, 2006.
- Pal, S. and Sharma, P.: A Review of Machine Learning Applications in Land Surface Modeling, *Earth*, 2, 174–190, 2021.
- 1090 Peckham, S. D., Hutton, E. W. H., and Norris, B.: A component-based approach to integrated modeling in the geosciences: The design of CSDMS, *Comput. Geosci.*, 53, 3–12, 2013.
- Penman, H. L. and Keen, B. A.: Natural evaporation from open water, bare soil and grass, *Proc. R. Soc. Lond. A Math. Phys. Sci.*, 193, 120–145, 1948.
- Pereira, L. S., Allen, R. G., Smith, M., and Raes, D.: Crop evapotranspiration estimation with FAO56: Past and future, *Agric. Water Manage.*,
- 1095 147, 4–20, 2015.
- Perrochet, P.: Water uptake by plant roots — A simulation model, I. Conceptual model, *J. Hydrol.*, 95, 55–61, 1987.
- Poggi, D., Katul, G. G., and Albertson, J. D.: A note on the contribution of dispersive fluxes to momentum transfer within canopies, *Bound.-Layer Meteorol.*, 111, 615–621, 2004.
- Porporato, A., Daly, E., and Rodriguez-Iturbe, I.: Soil water balance and ecosystem response to climate change, *Am. Nat.*, 164, 625–632,
- 1100 2004.
- Prentice, I. C., Liang, X., Medlyn, B. E., and Wang, Y.-P.: Reliable, robust and realistic: the three R’s of next-generation land-surface modelling, *Atmos. Chem. Phys.*, 15, 5987–6005, 2015.
- Priestley, C. H. B. and Taylor, R. J.: On the Assessment of Surface Heat Flux and Evaporation Using Large-Scale Parameters, *Mon. Weather Rev.*, 100, 81–92, 1972.
- 1105 Queloz, P., Bertuzzo, E., Carraro, L., Botter, G., Miglietta, F., Rao, P., and Rinaldo, A.: Transport of fluorobenzoate tracers in a vegetated hydrologic control volume: 1. Experimental results, *Water Resources Research*, 51, 2773–2792, <https://doi.org/10.1002/2014WR016433>, 2015.
- Rahman, J. M., Seaton, S. P., Perraud, J. M., Hotham, H., Verrelli, D. I., Coleman, J. R., and Others: It’s TIME for a new environmental modelling framework, in: MODSIM 2003 International Congress on Modelling and Simulation, vol. 4, pp. 1727–1732, 2003.
- 1110 Richards, L. A.: Capillary conduction of liquids through porous mediums, *Physics*, 1, 318–333, 1931.
- Richards, M. and Ford, N.: *Fundamentals of software architecture*, O’Reilly Media, Sebastopol, CA, 2020.
- Richardson, L. F.: *Weather Prediction by Numerical Process*, Cambridge University Press, 1922.
- Rigon, R., Bertoldi, G., and Over, T. M.: GEOTop: A Distributed Hydrological Model with Coupled Water and Energy Budgets, *J. Hydrometeorol.*, 7, 371–388, 2006.
- 1115 Rigon, R., Formetta, G., Bancheri, M., Tubini, N., D’Amato, C., David, O., and Massari, C.: HESS Opinions: Participatory Digital eARth Twin Hydrology systems (DARTHs) for everyone – a blueprint for hydrologists, *Hydrol. Earth Syst. Sci.*, 26, 4773–4800, 2022.

- Rouson, D., Xia, J., and Xu, X.: Scientific Software Design: The Object-Oriented Way, The object-oriented way, Cambridge University Press, Cambridge, England, 2014.
- 1120 Ryu, Y., Baldocchi, D. D., Kobayashi, H., van Ingen, C., Li, J., Black, T. A., Beringer, J., van Gorsel, E., Knohl, A., Law, B. E., and Roupsard, O.: Integration of MODIS land and atmosphere products with a coupled-process model to estimate gross primary productivity and evapotranspiration from 1 km to global scales, *Global Biogeochem. Cycles*, 25, 2011.
- Schröder, T., Javaux, M., Vanderborght, J., Körfgen, B., and Vereecken, H.: Effect of local soil hydraulic conductivity drop using a three-dimensional root water uptake model, *Vadose Zone J.*, 7, 1089–1098, 2008.
- 1125 Schymanski, S. J. and Or, D.: Leaf-scale experiments reveal an important omission in the Penman–Monteith equation, *Hydrol. Earth Syst. Sci.*, 21, 685–706, 2017.
- Serafin, F.: Enabling modeling framework with surrogate model- ing capabilities and complex networks, Ph.D. thesis, University of Trento, 2019.
- Silva, M., Matheny, A. M., Pauwels, V. R. N., Triadis, D., Missik, J. E., Bohrer, G., and Daly, E.: Tree hydrodynamic modelling of the soil–plant–atmosphere continuum using FETCH3, *Geoscientific Model Development*, 15, 2619–2634, 2022.
- 1130 Simard, S. W., Perry, D. A., Jones, M. D., Myrold, D. D., Durall, D. M., and Molina, R.: Net transfer of carbon between ectomycorrhizal tree species in the field, *Nature*, 388, 579–582, 1997.
- Staudinger, M., Stoelzle, M., Cochand, F., Seibert, J., Weiler, M., and Hunkeler, D.: Your work is my boundary condition!, *J. Hydrol.*, 571, 235–243, 2019.
- Stedle, E.: Water uptake by plant roots: an integration of views, *Plant Soil*, 226, 45–56, 2000.
- 1135 Tubini, N.: Theoretical and numerical tools for studying the Critical Zone from plot to catchments, Ph.D. thesis, University of Trento, 2021.
- Tubini, N. and Rigon, R.: Implementing the Water, HEat and Transport model in GEOframe (WHETGEO-1D v.1.0): algorithms, informatics, design patterns, open science features, and 1D deployment, *Geosci. Model Dev.*, 15, 75–104, 2022.
- Tubini, N., Gruber, S., and Rigon, R.: A method for solving heat transfer with phase change in ice or soil that allows for large time steps while guaranteeing energy conservation, *cryosphere*, 15, 2541–2568, 2021.
- 1140 Vereecken, H., Weihermüller, L., Assouline, S., Šimůnek, J., Verhoef, A., Herbst, M., Archer, N., Mohanty, B., Montzka, C., Vanderborght, J., Balsamo, G., Bechtold, M., Boone, A., Chadburn, S., Cuntz, M., Decharme, B., Ducharne, A., Ek, M., Garrigues, S., Goergen, K., Ingwersen, J., Kollet, S., Lawrence, D. M., Li, Q., Or, D., Swenson, S., Vrese, P., Walko, R., Wu, Y., and Xue, Y.: Infiltration from the pedon to global grid scales: An overview and outlook for land surface modeling, *Vadose Zone J.*, 18, 1–53, 2019.
- Verhoef, A. and Egea, G.: Modeling plant transpiration under limited soil water: Comparison of different plant and soil hydraulic parameter- izations and preliminary implications for their use in land surface models, *Agric. For. Meteorol.*, 191, 22–32, 2014a.
- 1145 Verhoef, A. and Egea, G.: Modeling plant transpiration under limited soil water: Comparison of different plant and soil hydraulic parameter- izations and preliminary implications for their use in land surface models, *Agric. For. Meteorol.*, 191, 22–32, 2014b.
- White, D. A., Beadle, C. L., Sands, P. J., Worledge, D., and Honeysett, J. L.: Quantifying the effect of cumulative water stress on stomatal conductance of *Eucalyptus globulus* and *Eucalyptus nitens*: A phenomenological approach, *Aust. J. Plant Physiol.*, 26, 17–27, 1999.
- 1150 Wilkinson, M. D., Dumontier, M., Aalbersberg, I. J. J., Appleton, G., Axton, M., Baak, A., Blomberg, N., Boiten, J.-W., da Silva Santos, L. B., Bourne, P. E., Bouwman, J., Brookes, A. J., Clark, T., Crosas, M., Dillo, I., Dumon, O., Edmunds, S., Evelo, C. T., Finkers, R., Gonzalez-Beltran, A., Gray, A. J. G., Groth, P., Goble, C., Grethe, J. S., Heringa, J., 't Hoen, P. A. C., Hooft, R., Kuhn, T., Kok, R., Kok, J., Lusher, S. J., Martone, M. E., Mons, A., Packer, A. L., Persson, B., Rocca-Serra, P., Roos, M., van Schaik, R., Sansone, S.-A., Schultes, E., Sengstag, T., Slater, T., Strawn, G., Swertz, M. A., Thompson, M., van der Lei, J., van Mulligen, E., Velterop, J., Waagmeester, A.,

- 1155 Wittenburg, P., Wolstencroft, K., Zhao, J., and Mons, B.: The FAIR Guiding Principles for scientific data management and stewardship, *Sci Data*, 3, 160018, 2016.
- York, L. M., Carminati, A., Mooney, S. J., Ritz, K., and Bennett, M. J.: The holistic rhizosphere: integrating zones, processes, and semantics in the soil influenced by roots, *J. Exp. Bot.*, 67, 3629–3643, 2016.
- 1160 Yu, L.-Y., Cai, H.-J., Zheng, Z., Li, Z.-J., and Wang, J.: Towards a more flexible representation of water stress effects in the nonlinear Jarvis model, *J. Integr. Agric.*, 16, 210–220, 2017.